J. Fluid Mech. (2004), *vol.* 516, *pp.* 39–82.
DOI: 10.1017/S0022112004000151 Printed in the United Kingdom

Aeroacoustics of hot jets

By K. VISWANATHAN

The Boeing Company, MS 67-ML, PO Box 3707, Seattle, WA 98124-2207, USA
k.viswanathan@boeing.com

(Received 23 July 2002 and in revised form 15 November 2003)

A systematic study has been undertaken to quantify the effect of jet temperature on the noise radiated by subsonic jets. Nozzles of different diameters were tested to uncover the effects of Reynolds number. All the tests were carried out at Boeing's Low Speed Aeroacoustic Facility, with simultaneous measurement of thrust and noise. It is concluded that the change in spectral shape at high jet temperatures, normally attributed to the contribution from dipoles, is due to Reynolds number effects and not dipoles. This effect has not been identified before. A critical value of the Reynolds number that would need to be maintained to avoid the effects associated with low Reynolds number has been estimated to be ~400 000. It is well-known that large-scale structures are the dominant generators of noise in the peak radiation direction for high-speed jets. Experimental evidence is presented that shows the spectral shape at angles close to the jet axis from unheated low subsonic jets to be the same as from heated supersonic jets. A possible mechanism for the observed trend is proposed. When a subsonic jet is heated with the Mach number held constant, there is a broadening of the angular sector in which peak radiation occurs. Furthermore, there is a broadening of the spectral peak. Similar trends have been observed at supersonic Mach numbers. The spectral shapes in the forward quadrant and in the near-normal angles from unheated and heated subsonic jets also conform to the universal shape obtained from supersonic jet data. Just as for unheated jets, the peak frequency at angles close to the jet axis is independent of jet velocity as long as the acoustic Mach number is less than unity. The extensive database generated in the current test programme is intended to provide test cases with high-quality data that could be used for the evaluation of theoretical/semi-theoretical jet noise prediction methodologies.

1. Introduction

The noise from heated jets has been measured since the early 1970s by several researchers, both in Europe and in the USA. From a survey of available data on jet noise a careful examination reveals that the database is by no means comprehensive and that the quality of the data is not uniformly high. Many fundamental questions on the noise of hot subsonic jets still remain unanswered, even after decades of study. For example, it has been believed widely by jet noise theoreticians that an extra source of noise, of the dipole type, is important at high temperatures, especially at low Mach numbers. Another question for which there is no unambiguous answer concerns the effect of jet density on noise at different jet velocities. The effects of Reynolds number of scale-model nozzles is rarely appreciated or investigated thoroughly. This study addresses these and several other issues. The effect of Reynolds number is evaluated through testing nozzles of different diameters at the same jet operating

conditions. Comparisons of these data, properly scaled, should uncover the effect of the Reynolds number explicitly. Many anomalous trends have been noted in the past experiments, due to a variety of problems with the test facilities and instrumentation. Noise from valves and combustors, flow noise due to high flow velocities in the ducts and sharp bends, and several other internal noise sources, have rendered much of the data hopelessly contaminated. It is extremely important to minimize rig noise. Measurement of noise at low jet velocities ($V_j/a \leqslant 0.6$, where a is the speed of sound in ambient air) poses a daunting challenge since the magnitude of the contamination could be much higher than the jet noise level. Great care has been taken to ensure good quality of data in the results reported here.

Bushell (1971) and Lush (1971) recognized the problems with existing data at that time and focused their efforts on acquiring clean jet noise data. The careful measurements of Lush established many of the noise characteristics of unheated jets. Ahuja (1973) confirmed these early results for unheated jets. The comment by Bushell (1971), "rig noise effects, which were unimportant at the higher exhaust velocities, become very important at low velocity, thus invalidating much of the research" is still very relevant. This statement was made just as high-bypass-ratio turbofan engines were being introduced, with the attendant low jet velocities. The large scatter seen in figure 1 of this reference highlights the problem with the quality of data available then. A more recent analysis of available jet noise data by Viswanathan (2003), carried out thirty years later, revealed severe problems with most recent data as well. Unfortunately, Bushell's comments are true even today. The tremendous advances in electronics and instrumentation now allow us to measure narrowband data to very high frequencies, while the early measurements were restricted to relatively low frequencies. Thus, we have the motivation and the means to clarify many long-standing issues in jet noise.

The study by Hoch *et al.* (1973) perhaps represents the first serious attempt at reconciling the conflicting data from earlier tests. A joint test program at the National Gas Turbine Establishment in England and SNECMA in France sought to clarify the effect of density on jet noise at various jet velocities. These measurements were made with convergent nozzles, with some of the test points at supercritical pressure ratios to obtain high jet velocities. Therefore, the contribution of shock noise was also included in their measured noise power when the nozzles were operated at supercritical pressure ratios. In order to investigate the effect of temperature on turbulent mixing noise alone, Tanna, Dean & Fisher (1975) and Tanna (1977) tested three convergent–divergent nozzles at their design Mach numbers of 1.4, 1.7, and 2.0, in addition to a convergent nozzle at subcritical pressure ratios. The results from these studies essentially confirmed the findings of Hoch *et al.* (1973) that the overall sound pressure levels increased with temperature at very low velocity ratios while the levels decreased at high velocity ratios, when the jet velocity was held constant. More recently, Seiner *et al.* (1992) carried out a detailed study of the effect of temperature on the noise of a perfectly expanded Mach 2.0 jet. This set of measurements provided valuable information on the directivity characteristics and established firmly that there is a dominant noise radiation sector, mainly confined to the aft angles. Outside this sector, the noise radiation was more or less uniform. These results played a large role in the development of the two similarity components of turbulent mixing noise, by Tam, Golebiowski & Seiner (1996). An experimental programme that aims to clarify the many issues discussed above has been completed, and a description of the programme and the salient results are presented below.

2. Experimental programme

In this study, we report the major findings from a comprehensive test programme carried out recently at the Low Speed Aeroacoustic Facility (LSAF) at Boeing. Detailed descriptions of the test facility, the jet simulator, the data acquisition and reduction process, etc., may be found in Viswanathan (2003). Hence, only an overview of the test is provided here. Both acoustic and thrust measurements were made simultaneously. The microphones were at a constant sideline distance of 15 ft (4.572 m) from the jet axis, except the microphone at 155°, which was at a distance of 12.75 ft (3.886 m). All angles are measured from the jet inlet axis, with a polar angular range of 50° to 155°. For some of the test points, additional microphones at a sideline distance of 9.17 ft (2.79 m) were also located at large polar angles so as to minimize interference with the exhaust collector; these microphones were at a different azimuthal angle. Bruel & Kjaer Type 4939 microphones (a newer type that replaced Type 4135) were used for free-field measurements. The microphones are set at normal incidence and without the protective grid, which yields a flat frequency response up to 100 kHz. Narrowband data with a bin spacing of 23.4 Hz were acquired and synthesized to produce 1/3-octave spectra, up to a centre band frequency of 80 000 Hz. The test matrix consisted of two series: for one set of data, the Mach number of the jet (or nozzle pressure ratio (NPR)) was held constant and the jet temperature was increased progressively. For the second set, data were acquired at constant jet velocities obtained through the proper choice of NPR and temperature ratio. An extensive database has been generated to answer many fundamental questions on the noise of hot jets as well as to provide high-quality data for the evaluation of prediction methods for jet noise.

3. Nozzle aerodynamics

The aerodynamic characteristics of a nozzle are reviewed briefly, before the examination of the noise characteristics. For a nozzle operating at a nozzle pressure ratio of (p_t/p_a) and reservoir temperature ratio of (T_t/T_a), the throat Mach number (M) is given by

$$M = \sqrt{\frac{2}{(\gamma-1)}\left[\left(\frac{p_t}{p_a}\right)^{\frac{\gamma-1}{\gamma}} - 1\right]} \quad \text{for} \quad \left\{\frac{p_t}{p_a}\right\} < \left(1+\frac{\gamma-1}{2}\right)^{\frac{\gamma}{\gamma-1}}, \tag{1}$$

$$M = 1 \quad \text{for} \quad \left(\frac{p_t}{p_a}\right) \geqslant \left(1+\frac{\gamma-1}{2}\right)^{\frac{\gamma}{\gamma-1}}. \tag{2}$$

From the gasdynamic equations, the expressions for the ideal mass flow rate $\dot{m}$, ideal jet velocity V_j, and ideal thrust F, may easily be derived in terms of the nozzle reservoir conditions:

$$\dot{m} = p_t A M \sqrt{\frac{\gamma}{RT_t}}\left[1+\frac{\gamma-1}{2}M^2\right]^{-\left(\frac{\gamma+1}{2(\gamma-1)}\right)}, \tag{3}$$

$$V_j = \sqrt{2RT_t\left(\frac{\gamma}{\gamma-1}\right)\left[1-\left\{\frac{p_t}{p_a}\right\}^{-\left(\frac{\gamma-1}{\gamma}\right)}\right]}, \tag{4}$$

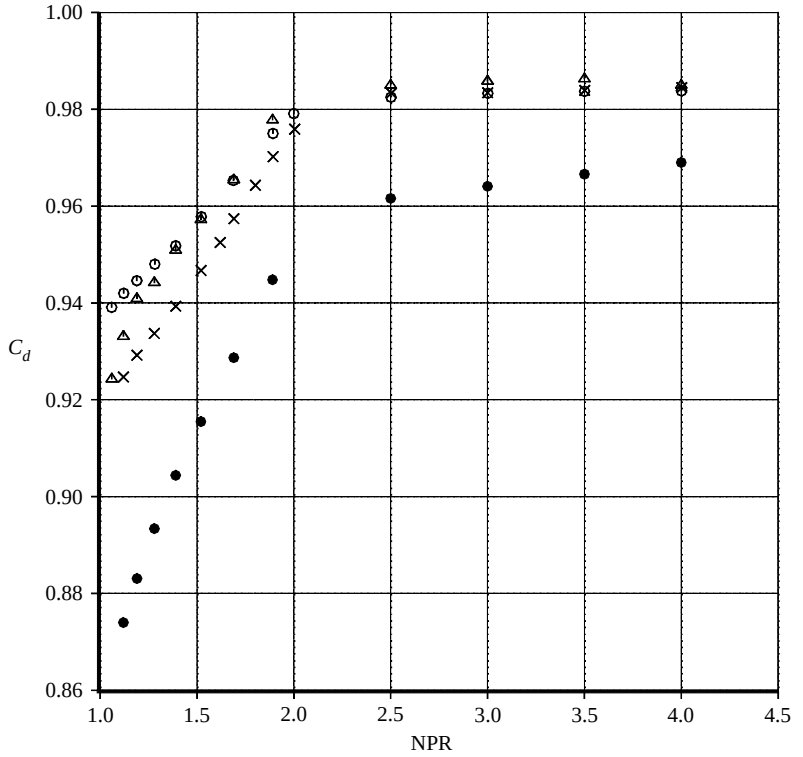

FIGURE 1. Variation of discharge coefficient with nozzle pressure ratio. ○, $D = 3.46$ in., $T_t/T_a = 1.0$; △, $D = 3.46$ in., $T_t/T_a = 3.2$; ×, $D = 1.5$ in., $T_t/T_a = 1.0$; ●, $D = 1.5$ in., $T_t/T_a = 3.2$.

$$F = \dot{m} V_j \tag{5}$$

$$= p_t A M \gamma \left[1 + \frac{\gamma - 1}{2} M^2\right]^{-\left(\frac{\gamma+1}{2(\gamma-1)}\right)} \sqrt{\left(\frac{2}{\gamma - 1}\right)\left[1 - \left\{\frac{p_t}{p_a}\right\}^{-\left(\frac{\gamma-1}{\gamma}\right)}\right]}. \tag{6}$$

In the above expressions, p_t is the plenum total pressure, A is the throat area, T_t is the plenum total or stagnation temperature, R is the gas constant, and γ is the ratio of specific heats.

In figure 1, the variation of the nozzle discharge coefficient (C_d), defined as the ratio of actual mass flow to ideal mass flow, with NPR is shown for two different nozzles of diameter 1.5 and 3.46 in. (3.81 and 8.79 cm). The variations are shown at two temperature ratios of 1.0 and 3.2. When the two cold cases are compared, denoted by the ○ and × in the figure, the effect of Reynolds number is readily apparent, with the smaller nozzle having lower values till the NPR reaches a value of ≈2. In the Reynolds numbers quoted here, the values of the kinematic viscosity are evaluated with the plenum stagnation conditions. When the jet is heated at a fixed NPR or Mach number, the Reynolds number decreases with increasing temperature. At the higher temperature ratio, the measured C_d values for the smaller nozzle decrease further, while the values for the larger nozzle is seen to decrease at low NPR. Thus, the aerodynamic characteristics are seen to be subject to the effects of Reynolds number. This is not a new result; similar trends have been observed for several

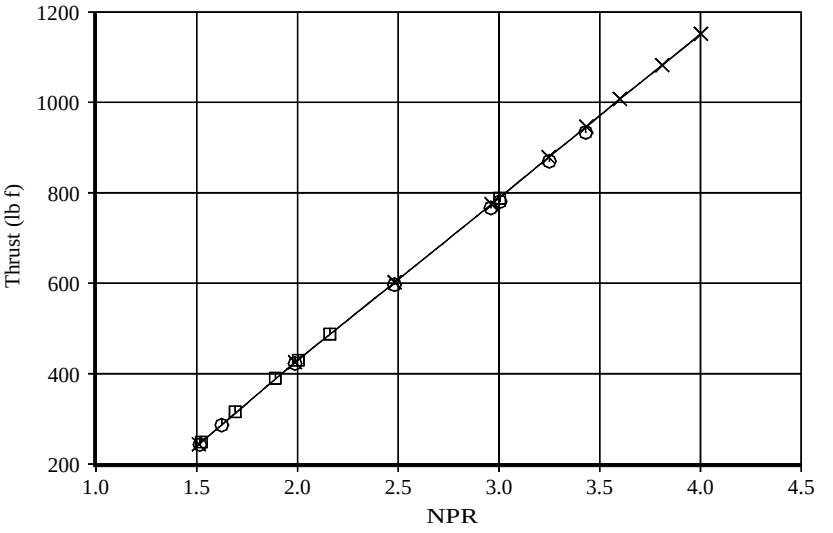

FIGURE 2. Variation of thrust with nozzle pressure ratio. ASME nozzle, $D = 4.93$ in.; ○, cold cycle; ×, hot cycle 1; □, hot cycle 2.

decades. However, this figure is included here to alert the reader to an unsuspected effect of Reynolds number on noise, which is addressed in the following sections.

In figure 2, the measured thrust from an ASME nozzle with diameter $D = 4.93$ in. (12.52 cm) is shown as a function of NPR. Three different engine cycles were tested: one was a cold cycle with the reservoir temperature equal to the ambient temperature (denoted by ○); the other two were typical engine cycles (× and □), with the maximum temperature reaching 944 K (1700°R). The solid line connects the data points for one of the hot cycles. The variation of the raw measured thrust, instead of the thrust coefficient, with NPR is plotted on the y-axis to explicitly bring out the effect of NPR on thrust. (For a typical variation of the thrust coefficient with NPR, see figure 8 in Viswanathan 2003). It is readily seen that the measured thrust at the different cycle points falls on a straight line and that the measured thrust is only a function of NPR. Examination of Equation (6) indicates that for a given nozzle, thrust is indeed a function of NPR. The jet total temperature has an indirect effect since γ is a function of temperature. When the jet is heated, the value of γ typically decreases. For the propane fuel used to heat the jet in the above experiments, the value of γ for the fuel/air mixture decreases from 1.4 at ambient temperature to approximately 1.34 at 944 K. This results in a decrease in thrust of $\approx$0.5% at a fixed NPR. Thus, the jet temperature has a weak effect on thrust.

A crucial point should be kept in mind when examining the effect of jet temperature on noise at fixed jet velocity. Clearly, the thrust level decreases as the nozzle pressure ratio is decreased and the temperature increased to produce the same jet velocity. Hence, comparisons of noise at fixed jet velocity are not made at constant thrust.

4. Acoustics

4.1. *Assessment of data quality*

First we address the issue of data quality, since this is of paramount importance in establishing the validity and interpretation of data. The high quality of acoustic data has been established through good agreement of the new data with those obtained

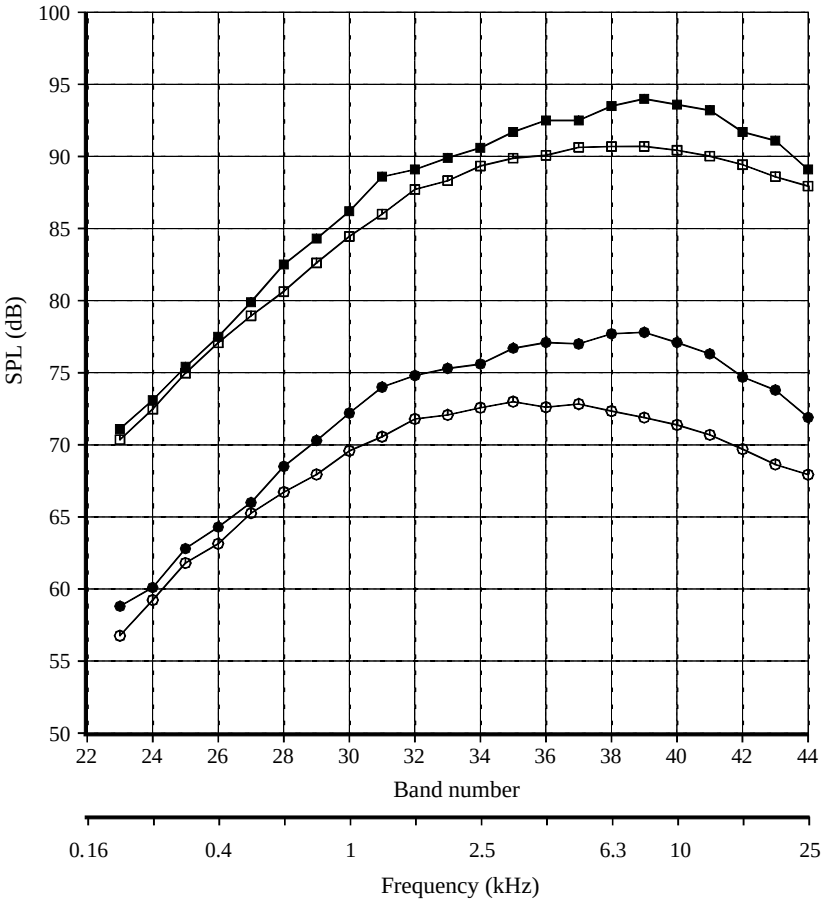

FIGURE 3. Comparison of current data with that of Ahuja (1973). Unheated jets, angle = 90°. Open symbols: current data ($D = 1.5$ in.); filled symbols: from Ahuja (1973) ($D = 1.52$ in.). ○, ●: $V_j = 600\,\text{ft s}^{-1}$; □, ■: $V_j = 1000\,\text{ft s}^{-1}$.

with a blow-down tunnel using the same nozzles, as reported in Viswanathan (2003). Additional comparisons with data acquired at other facilities and published in the literature are shown now. Figures 3 and 4 show spectral comparisons with data from Ahuja (1973). Three nozzles of diameters 1.52, 2.4 and 2.84 in. (3.86, 6.1 and 7.2 cm) were used in the measurements carried out at the National Gas Turbine Establishment (NGTE, Pyestock). In the present study, three nozzles of diameters 1.5, 2.45 and 3.46 in. (3.81, 6.2 and 8.79 cm) were used. In figure 3, spectra at 90° from the smallest nozzle from unheated jets at two velocities of 600 and 1000 ft s^{-1} are shown. The effect of the small discrepancy in the sizes (1.52 and 1.5 in.) results in a difference of 0.12 dB in level, which has been accounted for. However, the minor difference in Strouhal number is ignored and raw frequencies are used on the x-axis, since it does not change the main result. The current data have been corrected to a polar arc of 6 feet and to standard day conditions (59 °F and 70% relative humidity) to facilitate direct comparison with the NGTE data. The atmospheric attenuation is calculated using the method of Shields & Bass (1977). Figure 3 indicates that the levels of the NGTE are higher than the current ones, with the discrepancy more pronounced at the higher frequencies. Furthermore, the magnitude of the elevated

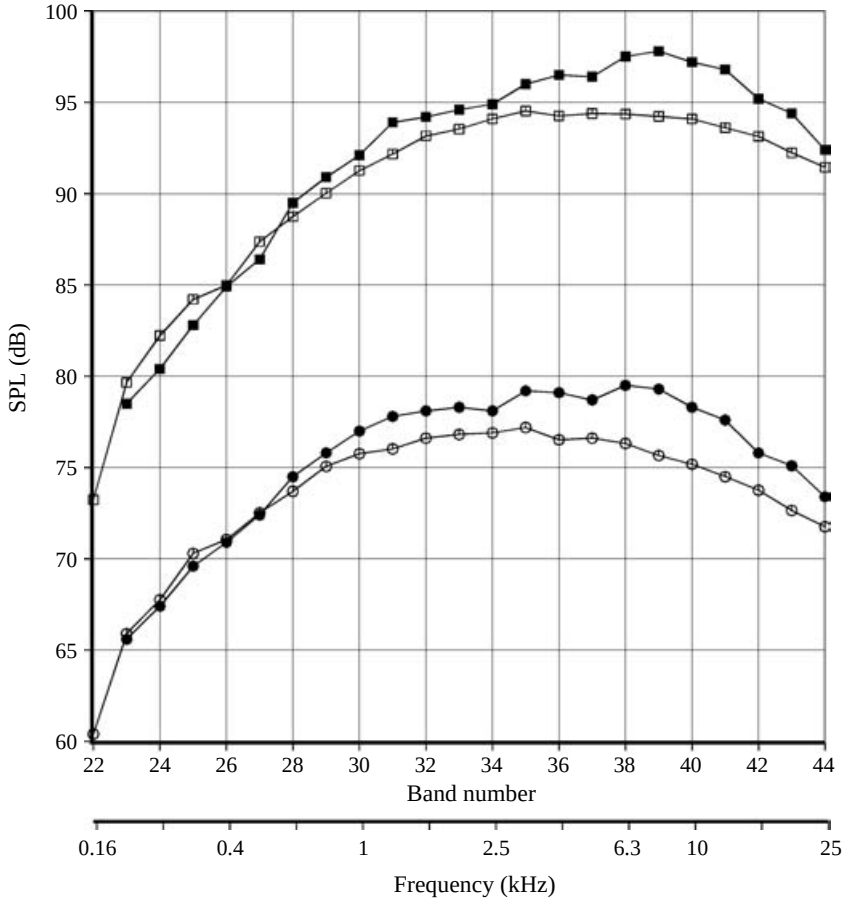

FIGURE 4. As figure 3 but for current data $D = 2.45$ in. and Ahuja (1973) $D = 2.4$ in.

levels from NGTE is $\sim$5 dB at the lower jet velocity and becomes smaller at the higher jet velocity. A similar comparison is shown in figure 4 with the larger nozzles of 2.4 and 2.45 in. diameters, respectively. Once again, similar trends are observed with the levels of the NGTE data being higher at higher frequencies. As was done in figure 3, the effect of the different diameters was accounted for in amplitude while neglecting the small effect on Strouhal number. Comparisons at other jet velocities (not shown here) also indicated elevated levels for the NGTE data for nozzles of both sizes.

A detailed discussion of the impact of the nozzle size on data quality was provided in Viswanathan (2003). It was shown with concrete examples that the spectra from a larger nozzle are subject to higher levels of contamination from internal noise, especially at lower Mach numbers. Rig noise, which is a function of a high exponent of internal velocity, is more pronounced for larger nozzles for the following reason. For a fixed jet velocity at the nozzle exit, the internal velocity is higher so as to accommodate the higher mass flow for a larger nozzle. Even though the larger nozzle generates more pure jet noise, the strength of the internal noise increases at a much faster rate thereby compromising the quality of data. The importance of understanding the rig constraints in choosing the proper size of the nozzle so as to avoid measuring contaminated data from a given compact rig was emphasized. It was

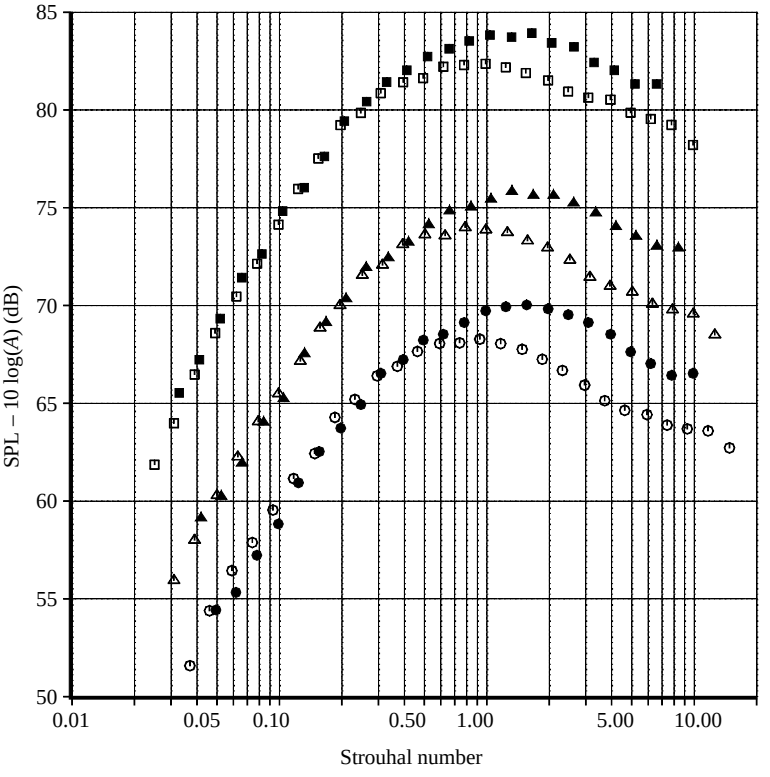

FIGURE 5. Comparison of data from Tanna *et al.* (1975) and Tanna (1977) (referred to as Tanna's data in what follows) with current data. Unheated jets, angle = 90°. Open symbols: current data ($D = 1.5$ in.); filled symbols: Tanna's data. ○, ●, $M = 0.62$; △, ▲, 0.74; □, ■, 0.98.

pointed out that the current data obtained with the nozzle of 2.45 in. diameter had a contamination of ~3 dB at the higher frequencies for cold jets at the lower jet velocity of 600 ft s^{-1} ($M = 0.55$). Therefore, the levels of the NGTE data for the larger nozzle could be off by more than 5 dB at the higher frequencies for the lower jet velocity.

Next we show comparisons with the data acquired by Tanna *et al.* (1975) and Tanna (1977) (referred to hereafter as Tanna's data). A 2.0 in. nozzle was used in their tests and data were acquired on a 12 ft (3.658 m) polar microphone array. The 1/3-octave data were reported in lossless form. To facilitate one-to-one comparison, the current data (with $D = 1.5$ in.) have been corrected to lossless form on a polar arc of 12 ft (3.658 m). The effect of the nozzle size on spectral levels has been removed through the subtraction of $[10 \log_{10}(A)]$. Hence the levels should be interpreted as the noise per unit area.

The frequencies have been converted to Strouhal numbers. Spectral comparisons at 90°, for three Mach numbers of 0.62, 0.74 and 0.98 are shown in figure 5. While there is good agreement at the lower frequencies, the spectral levels of Tanna's data are again higher than the current data at the higher frequencies. As seen in figures 3 and 4, the magnitude of the discrepancy is more pronounced at lower Mach numbers. These three figures suggest that the spectra from these two facilities could be contaminated by extraneous noise.

A popular misconception relates to the contraction ratio of the upstream plumbing to that of the nozzle being tested. It was believed that having a large contraction

ratio ensured good quality of noise data. However, this is not so. Improper fittings, gaps, steps, screw heads, etc., downstream of the plenum could easily vitiate quality. Viswanathan (2003) showed unambiguously that it is possible to acquire data with a compact rig that is almost as good in quality as that obtained with a blow-down tunnel, provided care is taken in the proper design of the rig, selection of nozzle size, etc. For the sake of perspective, it is noted that the contraction ratios in the current compact rig for the primary and secondary streams were 10.7 and 3.6, for the spectral comparisons from dual-stream nozzles provided in Viswanathan (2003). In contrast, the two streams were fed by independent plenum tanks in the blow-down rig. Let us re-examine figures 3 and 4. The contraction ratios in the NGTE tests for the two nozzles were 250 and 100, while they were 28 and 10.7 in the current test. However, the NGTE data have higher levels and the spectra are not as smooth. The variation in the magnitude of the noise contamination with jet velocity is a good indicator of the influence of rig internal noise. These two instances indicate clearly that a large contraction ratio by itself does not guarantee good data.

The problems in the spectra from three other facilities were described in Viswanathan (2003). Given the poor quality of these data as well, the current data were benchmarked against those from a blow-down facility with good agreement, as described in the above reference. Thus, every effort has been made to assess the current data. Hence, there should be no questions as to the goodness of the data or the validity of the conclusions drawn here. Discussion of the implications of the potential contamination in the above two sets of data is deferred till a later section.

4.2. *Spectral characteristics at radiation angles near 90 degrees*

The salient noise characteristics are now presented. First, it is shown that the measured spectra with nozzles of different diameters do collapse when properly scaled. Normalized spectra from three conic nozzles of diameters 1.5, 2.45 and 3.46 in. at a radiation angle of 90° are presented in figure 6(*a*). The spectra are normalized as follows: the effects of jet velocity and the nozzle diameter on spectral levels are scaled out. The parameter $(\mathrm{SPL} - 80\log_{10}(V_j/a) - 10\log_{10}(A))$ is plotted against the Strouhal number at five Mach numbers of 0.6, 0.7, 0.8, 0.9 and 1.0. The open symbols represent spectra from the nozzle with $D = 1.5$ in., the filled symbols from $D = 2.45$ in. and the numbers from $D = 3.46$ in. There is very good collapse of the spectra at the lower frequencies and near the peak. The scatter in the data up to a Strouhal number of 4.0 is $\sim$1 dB. At the higher Strouhal numbers, the spectra from the largest nozzle have elevated levels, which continue to increase with increasing frequency. The symbols for the spectra from the nozzle of diameter $D = 3.46$ in. have been selected in reverse order (5 for $M = 0.6$, 1 for $M = 1.0$). We symbolically denote that the level of contamination is more pronounced at lower jet velocities (Mach numbers), which is expected. Two important conclusions are drawn from this figure: (*a*) rig noise is mostly confined to the higher frequencies, well above the peak frequency; (*b*) there is no near-field effect for the largest nozzle, since there is excellent collapse of the spectra at the lowest frequencies. This figure frames the issue of rig noise in a quantitative fashion.

In figure 6(*b*), a spectral comparison at an angle of 145° from a heated jet of Mach number 0.8 and a temperature ratio of 2.2 is presented. The 1/3-octave spectra have been corrected to a common distance of 20 ft and to lossless form. There is excellent agreement over the entire frequency range for this particular test point. However, as shown later, this level of agreement is possible only if the Reynolds number is above a certain value and if there is no contamination by rig noise. In figure 7, the

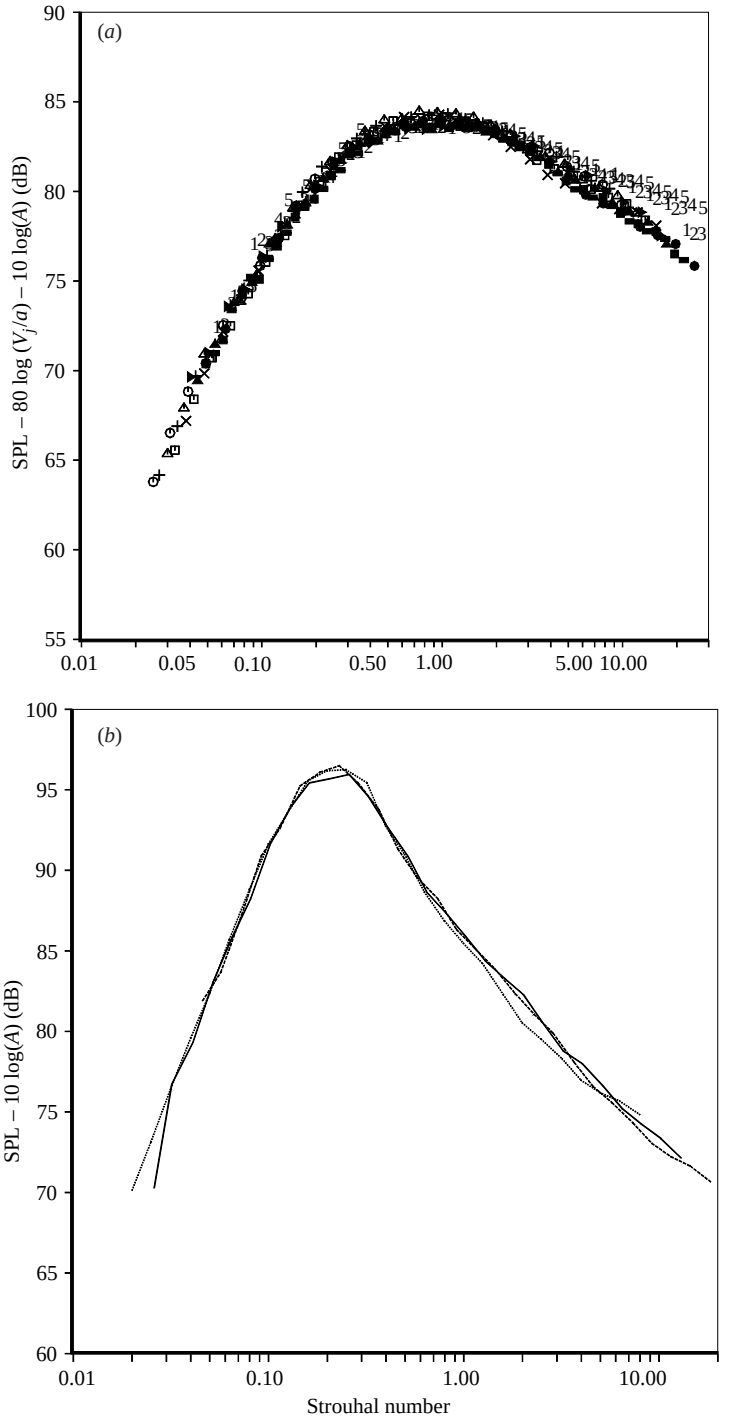

FIGURE 6. Measured spectra with nozzles of different diameters. (*a*) Unheated jets, angle = 90°. $M = 0.6$, 0.7, 0.8, 0.9, 1.0. Open symbols: $D = 1.5$ in.; filled symbols: $D = 2.45$ in.; numbers: $D = 3.46$ in. (*b*) $M = 0.8$, $T_t/T_a = 2.2$, angle = 145°. Dotted line: $D = 1.5$ in.; solid: 2.45 in.; dashed: 3.46 in.

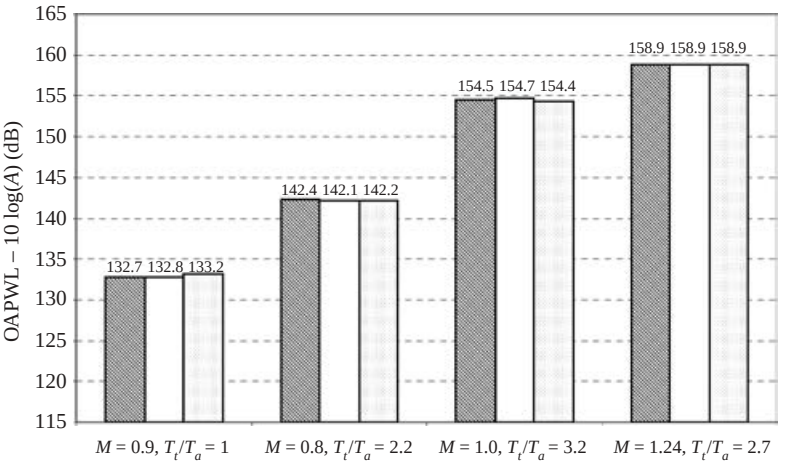

FIGURE 7. Overall power radiated by nozzles of different diameters at various cycle conditions. Hatched: $D = 1.5$ in.; blank: 2.45 in.; dots: 3.46 in.

radiated acoustic power at different cycle conditions obtained with the three nozzles is displayed. The acoustic power is quoted in dB relative to 10^{-12} W. Again, there is very good agreement in the overall power level at all the cycle conditions. In the above two figures, the effect of the nozzle size on spectral levels has been removed through the subtraction of $[10 \log_{10} (A)]$. The effect of nozzle size on the quality of noise data, discussed in detail in Viswanathan (2003), should be kept in mind especially when examining data at lower velocities. The above figures provide assurance that rig noise is not a problem at these conditions.

The spectral shape of unheated jets is now presented. Figure 8 shows a comparison of the measured spectra ($D = 1.5$ in.) at 90° and the fine-scale similarity (FSS) spectrum of Tam *et al.* (1996), from unheated jets at Mach numbers of 0.3, 0.4, 0.5, 0.6, 0.7, 0.8, 0.9, and 1.0. The curves have been spaced apart to enhance visual observation and the maximum spectral level associated with each curve is noted in all the figures. The peaks of the similarity spectra are placed on top of the peaks of the measured spectra in the following figures. This fitting method is not to be confused with the prediction method of Tam & Auriault (1999). The significance of an important effect, due to atmospheric attenuation, on the shapes of the similarity spectra was discussed in depth in Viswanathan (2002). It was pointed out that there is no easy fix for the omission of this effect and it was recommended that the shape of the universal spectrum at the higher frequencies be re-determined from data normalized to standard conditions. However, the universal shape as determined by Tam *et al.* (1996) is employed in the following sections, while fully recognizing the effect of atmospheric attenuation on spectral shapes at the higher frequencies. Therefore, as-measured data are used when making qualitative comparisons with the similarity spectra. Data corrected to standard day or lossless conditions are shown when direct comparisons are made. There is excellent agreement for Mach numbers 0.6 and higher. However, at a Mach number of 0.5, the data at the highest frequencies are slightly higher than the empirical curve. At $M = 0.4$, the discrepancy is more pronounced and the spectrum starts deviating above a frequency of 20 000 Hz (band # 43, where band # $= 10 \times \log_{10} (f)$, f being frequency in Hz.). The spectrum for $M = 0.3$ does not resemble that of jet noise at all and is corrupted completely by rig noise.

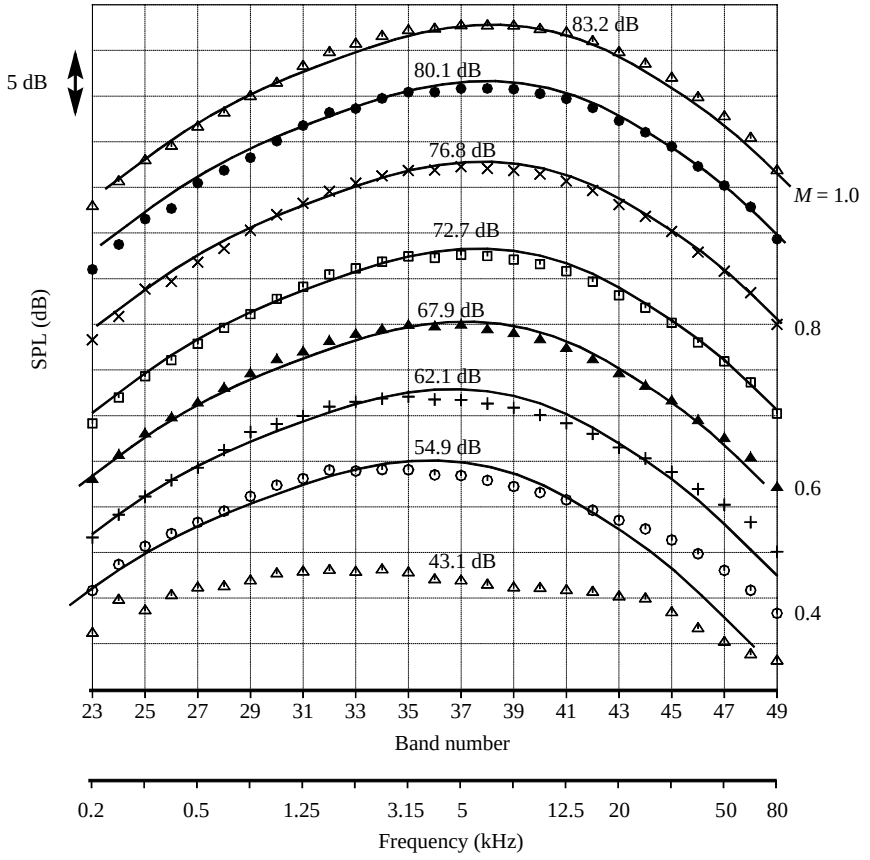

FIGURE 8. Comparison of spectra from cold jets. $D = 1.5$ in., angle $= 90°$. Symbols: $M = 0.3$, 0.4, 0.5, 0.6, 0.7, 0.8, 0.9, 1.0; lines: FSS spectrum.

Let us now examine the effect of temperature on jet noise. The measured spectra at 90° ($D = 1.5$ in.) at various temperatures ($T_t/T_a = 1.0$, 1.8, 2.2, 2.7, 3.2) are shown for a $M = 0.5$ and $M = 0.6$ jet in figures 9 and 10, respectively. Also shown in these figures are comparisons with the fine-scale similarity spectrum. Again, the curves have been spaced apart to enhance visual observation and do not reflect the noise increase due to heating. For the lower Mach number jet, there is a slight noise contamination at the higher frequencies, evident especially for the unheated case. As can be seen, when the jet is heated at these low Mach numbers, the spectral shape changes. For the unheated cases there is excellent agreement with the FSS spectrum, as also seen in figure 8. However, for the heated cases, the peak frequency shifts to lower values and there is an extra hump near the peak, which is more pronounced at the higher temperatures.

Many researchers in the past have proposed that the source of jet noise consists of quadrupoles and dipoles, with the contributions of dipoles pronounced at high jet temperatures, see for example figure 8 in Fisher *et al.* (1973). Based on observations similar to those seen in figures 9 and 10 in the data of Tanna and others, Tester & Morfey (1976) and Morfey, Szewczyk & Tester (1978) developed master spectra for the noise generated by quadrupole and dipole sources. The diameter of the nozzle in the above experiments was 2.0 in. For cold and isothermal jets, the noise was

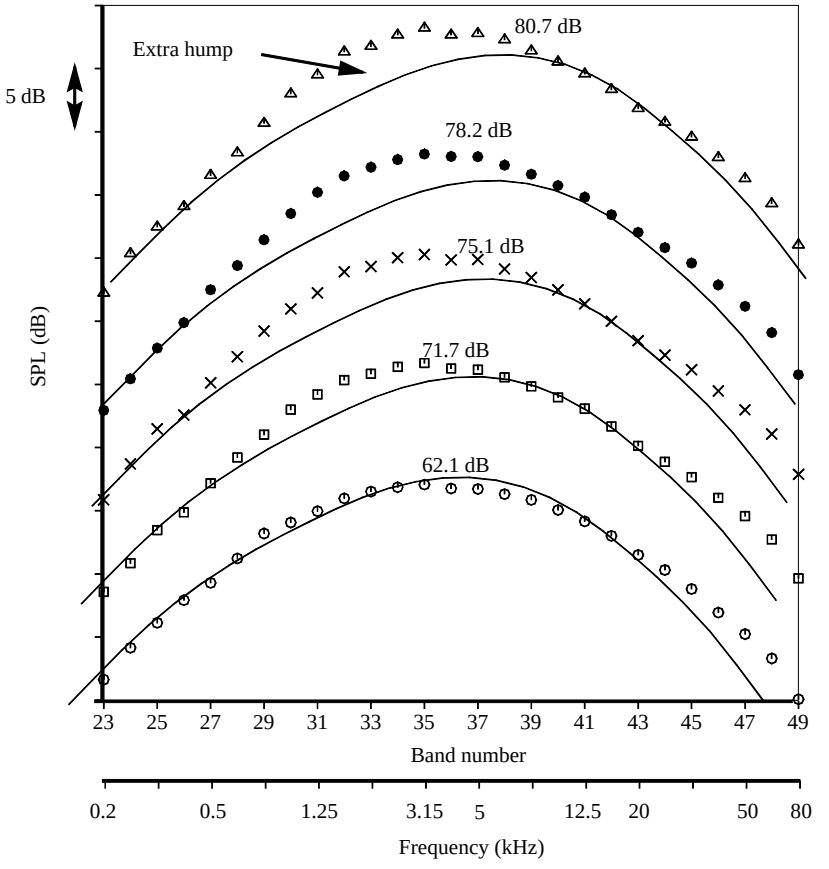

FIGURE 9. Comparison of measured spectra with fine-scale similarity spectrum. $M = 0.5$, angle $= 90°$, $D = 1.5$ in.; ○, $T_t/T_a = 1.0$; □, 1.8; ×, 2.2; ●, 2.7; △, 3.2.

modelled as being dominated by the quadrupole sources. The additional noise caused by the effect of heating the jet was then represented by temperature fluctuation terms of dipole order. The master spectra for the quadrupole and dipole sources at 90°, where convection and refraction effects are minimal, had different shapes, with the peak frequency for the dipole term lower than that for the quadrupole term. The master spectra are reproduced here in figure 11, along with the fine-scale similarity spectrum. Note the extra hump attributed to the dipole spectrum. The spectral levels in this figure are arbitrary and the actual noise levels are obtained through appropriate scaling. The dipole spectrum moves up and down relative to the quadrupole spectrum, according to (*a*) the difference in density between the jet and the ambient air, and (*b*) the jet velocity ratio (V_j/a). There is excellent agreement between the quadrupole spectrum and the FSS spectrum at the lower frequencies. The discrepancy at the higher frequencies is due to the following two reasons: first, the master spectra are in lossless form while the FSS spectrum was derived from as-measured data; secondly, the master spectra based on the data of Tanna are potentially affected by rig noise at the higher frequencies as shown in figure 5 and discussed in § 4.4. Many in the jet noise community have accepted this view of the noise generation mechanisms for hot jets for the past 25 years.

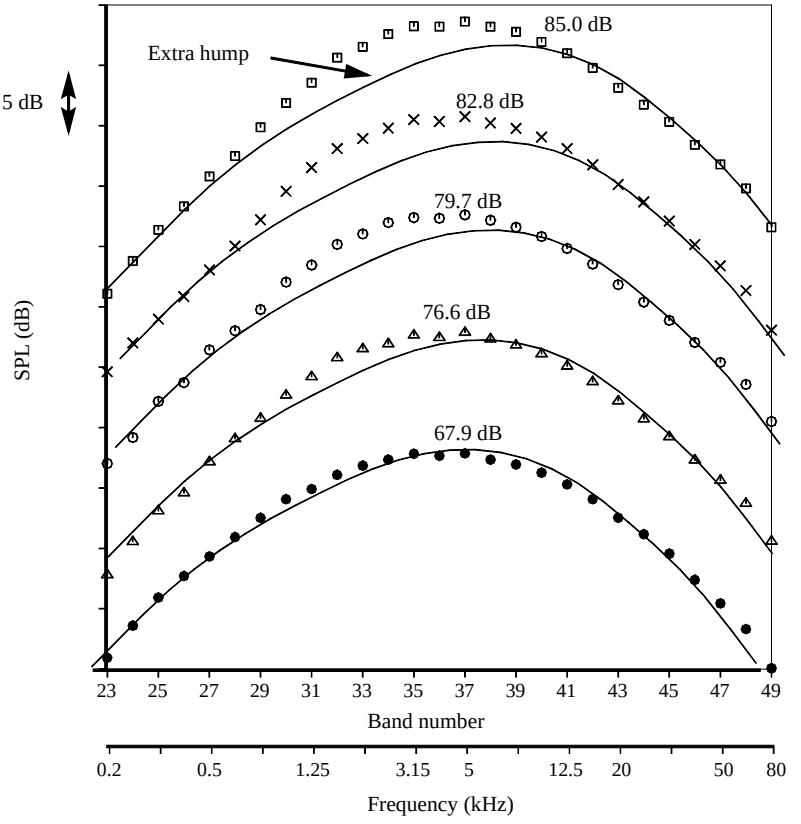

FIGURE 10. As figure 9 but for $M = 0.6$, ●, $T_t/T_a = 1.0$; △, 1.8; ○, 2.2; ×, 2.7; □, 3.2.

Let us now see if there is an alternative explanation. The spectra shown in figures 9 and 10 are now acquired with larger nozzles. Figures 12(*a*)–12(*c*) show similar comparisons between the measured spectra and the FSS spectrum for a Mach 0.6 jet ($D = 2.45$ in.) at three angles of 70°, 90°, and 100°, respectively. For this larger nozzle, rig noise adds a few dB to the spectra at the higher frequencies as seen in the discrepancy with the FSS spectrum, again more distinguishable for the unheated case. However, let us concentrate our attention near the peak frequency. There is excellent agreement with the FSS spectrum and the spectral shape does not change even at the higher temperatures. The humps seen in figures 9 and 10 are either completely absent or only barely discernible at the two higher temperature ratios at all three angles shown. Similar trends are observed at other Mach numbers as well. Figure 13 shows another comparison at 90° with a nozzle of diameter 3.46 in., at a Mach number of 0.6. Once again the agreement with the FSS spectrum is very good at the higher temperatures and there is no change in spectral shape due to heating.

Figures 14 and 15 show spectra at 90°, at various Mach numbers and at a temperature ratio of 3.2, from two nozzles of diameters 1.5 and 3.46 in., respectively. In figure 14, one can see the extra hump, the magnitude of which is more pronounced at lower Mach numbers. In figure 15, with $D = 3.46$ in., the spectral shapes conform to that of the FSS spectrum and there are no humps. This is the case even for a Mach number of 0.4, for which one would expect the extra noise source if it were actually present. It is recognized that the higher frequency portion of the spectrum at

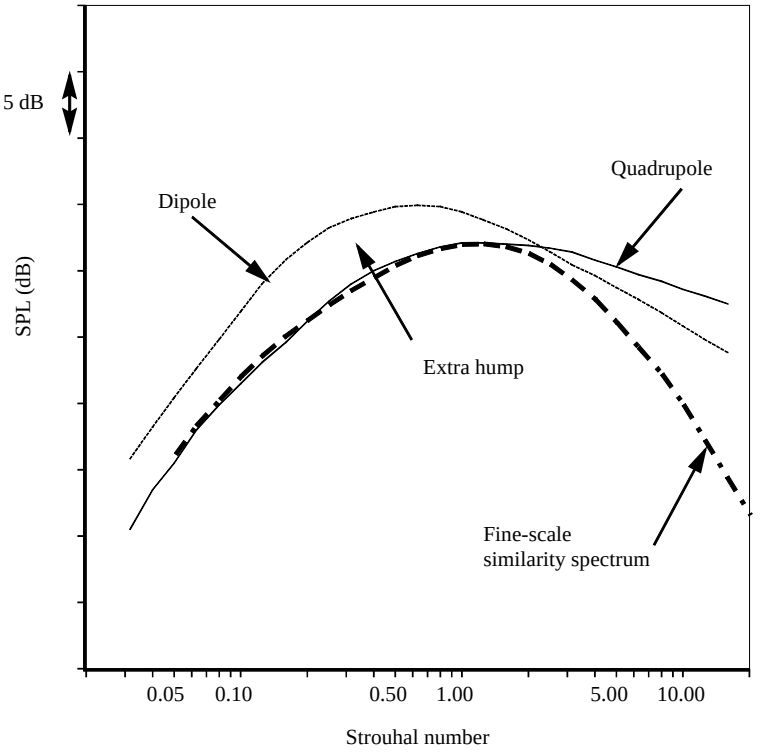

FIGURE 11. Comparison of master spectra.

$M = 0.4$ has some rig noise contamination; however, that is not the main issue here. For a comprehensive treatment of rig noise, especially for cold jets, see Viswanathan (2003).

Figure 16(*a*) summarizes the above findings and brings out the effect of Reynolds number explicitly. The spectra at 90° from a jet of Mach number 0.7 and temperature ratio 3.2 from three nozzles of diameters 1.5, 2.45 and 3.46 in. and comparisons with the FSS spectrum are shown. The extra hump is obvious in the spectra obtained with the smallest nozzle ($D = 1.5$ in.). The magnitude of the discrepancy between the data and the similarity spectrum near the spectral peak decreases for the nozzle with $D = 2.45$ in. and almost completely disappears for the largest nozzle. The only parameter different in the three cases is the Reynolds number, with values of 204 000, 333 200 and 470 600 for the three nozzles, respectively.

The author recognizes that this method of identifying the hump through comparison with the FSS is somewhat subjective. However, this issue is put on a firmer footing as follows. First, the effects of jet velocity (V_j/a) and nozzle diameter are scaled out from the spectra. Specifically, the variation of the normalized spectra with Strouhal number is examined. An exponent of 5.53 has been obtained for the velocity dependence at 90°, as discussed in § 4.5 and figure 32. The normalized spectra are presented in figure 16(*b*). The spectra obtained with the smaller nozzle ($D = 1.5$ in.) and denoted by the open symbols collapse to a single curve. The spectra for the larger nozzle ($D = 3.46$ in.), denoted by the filled symbols, collapse on to a different curve. The biggest difference between these two families of curves occurs near the spectral peak and at Strouhal numbers slightly lower than the peak, with the normalized levels

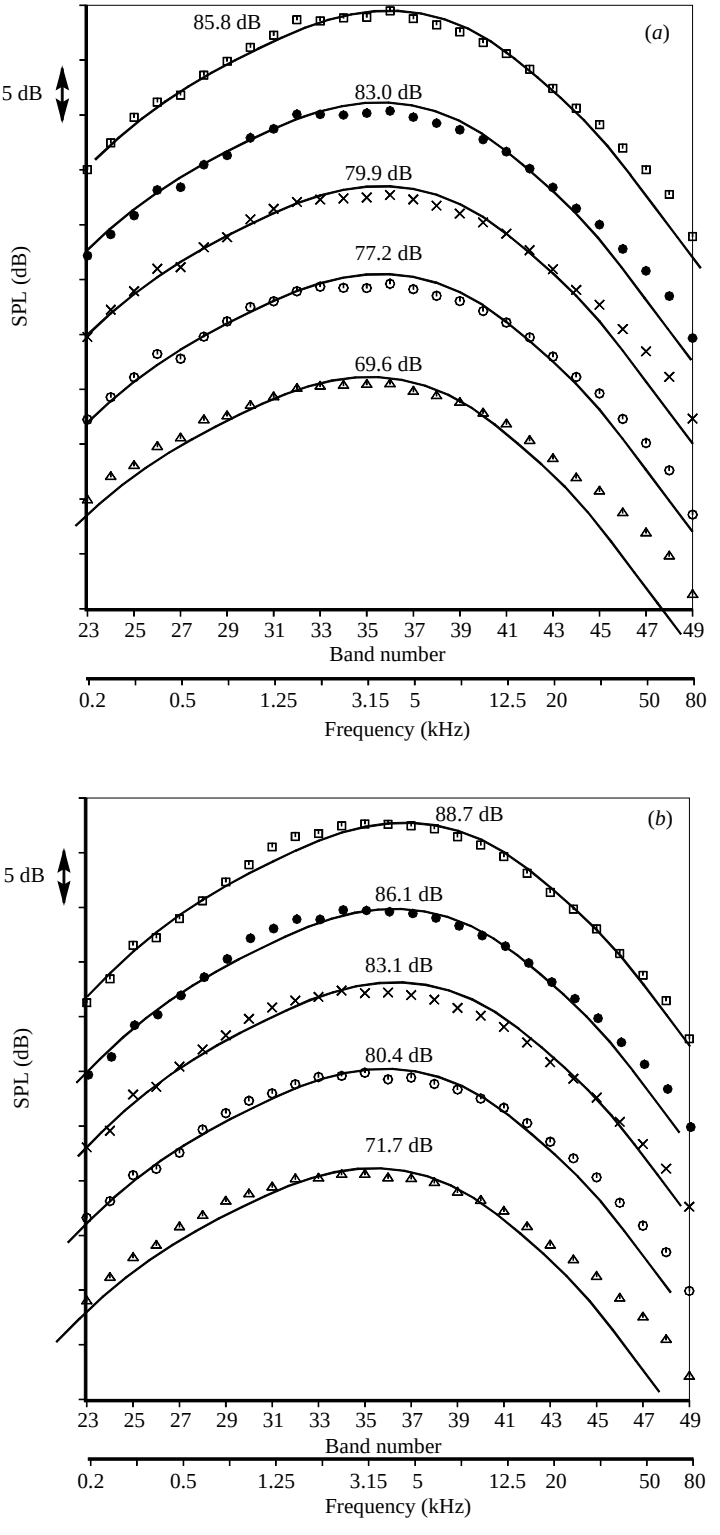

FIGURE 12(*a*, *b*). For caption see facing page.

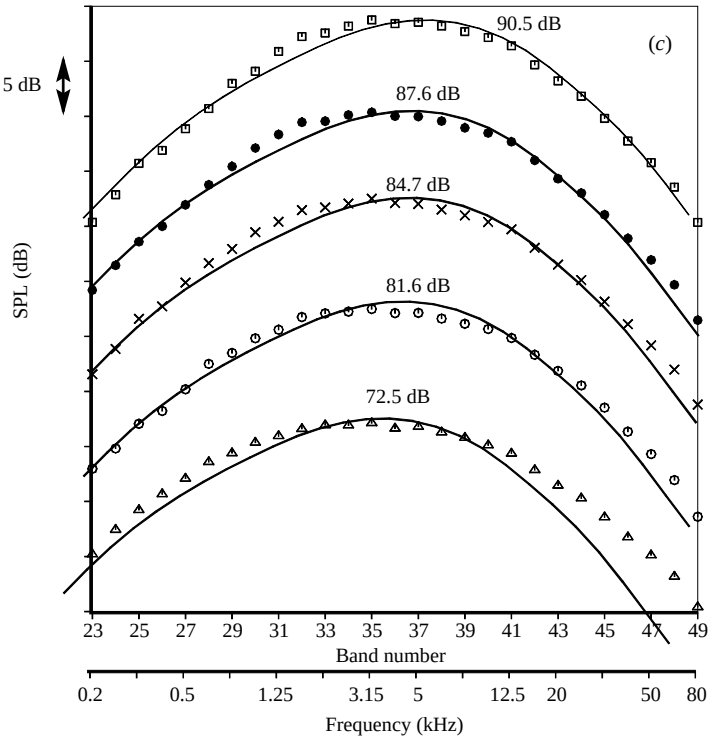

FIGURE 12. Comparison of measured spectra with fine-scale similarity spectrum. $M = 0.6$, $D = 2.45$ in. △, $T_t/T_a = 1.0$; ○, 1.8; ×, 2.2; ●, 2.7; □, 3.2. (*a*) 70°; (*b*) 90°; (*c*) 100°.

being higher for the smaller jet. This trend, suggested by figures 14 (with humps at all Mach numbers) and 15 (no such humps), shows up clearly when the spectra are compared on a common basis. Let us turn our attention to the higher Strouhal numbers and examine the spectral values for the $M = 0.5$ jets. The maximum value for the Strouhal number for the smaller nozzle is ~8 (for $f = 80$ kHz), denoted by the last open circle in figure 16(*b*). The spectral level for the larger nozzle (denoted by the filled circles) at the same Strouhal number is higher by ~2 dB. The discrepancy between the FSS and the spectrum for $M = 0.5$ in figure 15 at the corresponding frequency (~35 kHz) is again ~2 dB. Thus, the comparisons of the normalized spectra enable us to quantify the Reynolds number effects and the influence of the rig noise in a transparent manner.

Many theoreticians of jet noise maintain that an extra source of noise of the dipole type is important at high temperatures, especially at low Mach numbers. As seen in figure 11, the dipole contribution was thought to cause the extra hump in the spectra from heated jets. In figures 9, 10, and 12–16 we notice the supposed presence of dipoles in the spectra obtained with the smallest nozzle ($D = 1.5$ in.) while there is no evidence of dipoles in the noise of larger nozzles. Obviously, the extra hump seen with small nozzles is due to Reynolds number effects as demonstrated in figure 16(*a*, *b*) and has nothing to do with the presence of dipoles. It is worth reiterating the point that the Reynolds number decreases with increasing temperature, when a jet is heated at a fixed Mach number.

Why does the FSS spectrum fit the measured data without the extra hump? Tam *et al.* (1996) originally developed the empirical shapes from supersonic jet

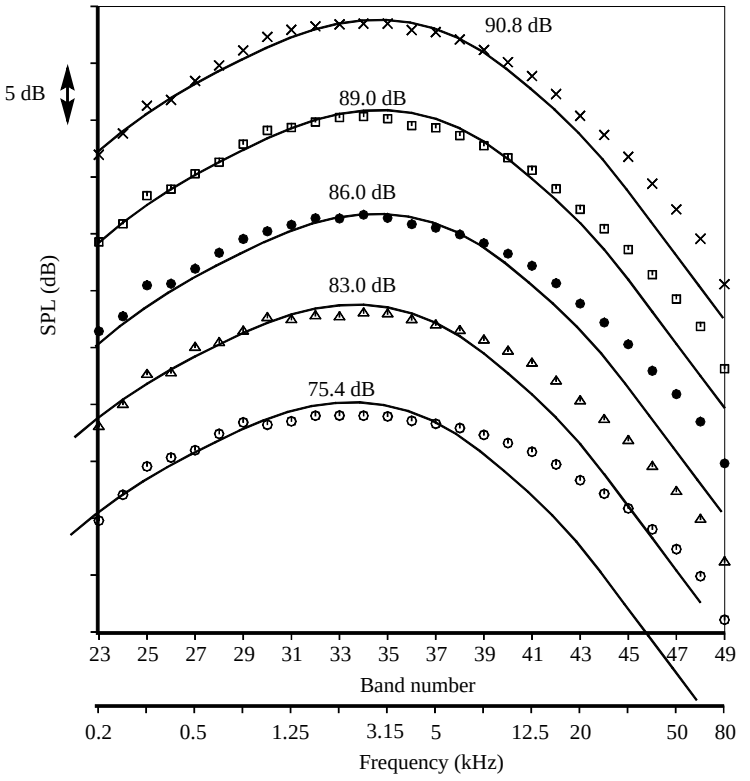

FIGURE 13. Comparison of measured spectra with fine-scale similarity spectrum. $M = 0.6$, angle $= 90°$, $D = 3.46$ in. ○, $T_t/T_a = 1.0$; △, 1.8; ●, 2.2; □, 2.7; ×, 3.2.

noise spectra; the Reynolds numbers of these jets are high even at highly elevated temperatures and therefore the spectra are not subject to the effect identified here. In fact, Tam *et al.* (1996) did not consider subsonic heated jets. Viswanathan (2002) was the first to show that the spectra from subsonic heated jets also conform to the universal shape; see figures 15 and 16 in that reference. From a comprehensive analysis of a large number of spectra at various angles and jet cycle conditions, and the sample results shown here and in Viswanathan (2002), it is established that there is no change in spectral shape due to heating as long as the Reynolds number is maintained above a certain value. Some have argued that dipoles do not radiate noise at 90° to the jet axis. To address this concern, excellent agreement of the measured spectra from hot jets with the FSS spectrum at other angles was shown in figures 12(*a*) and 12(*c*) above, and in figures 15 and 16 in Viswanathan (2002). Hence, it has been demonstrated that the spectral shapes do not change at other angles if the effects due to low Reynolds number are avoided.

A comparison of the radiated overall power at various Mach numbers and at a temperature ratio of 3.2 from two nozzles of diameters 1.5 and 2.45 in. is shown in figure 17. As can be seen, the smaller nozzle produces more noise (on an area-normalized basis) than the bigger nozzle, till a supersonic Mach number is reached. The contribution of shock noise becomes pronounced then and the Reynolds number is relatively high. Thus, a lower Reynolds number jet is seen to produce more noise, especially at low subsonic Mach numbers. An important issue that needs to be resolved is the question of whether temperature/density fluctuations due to heating

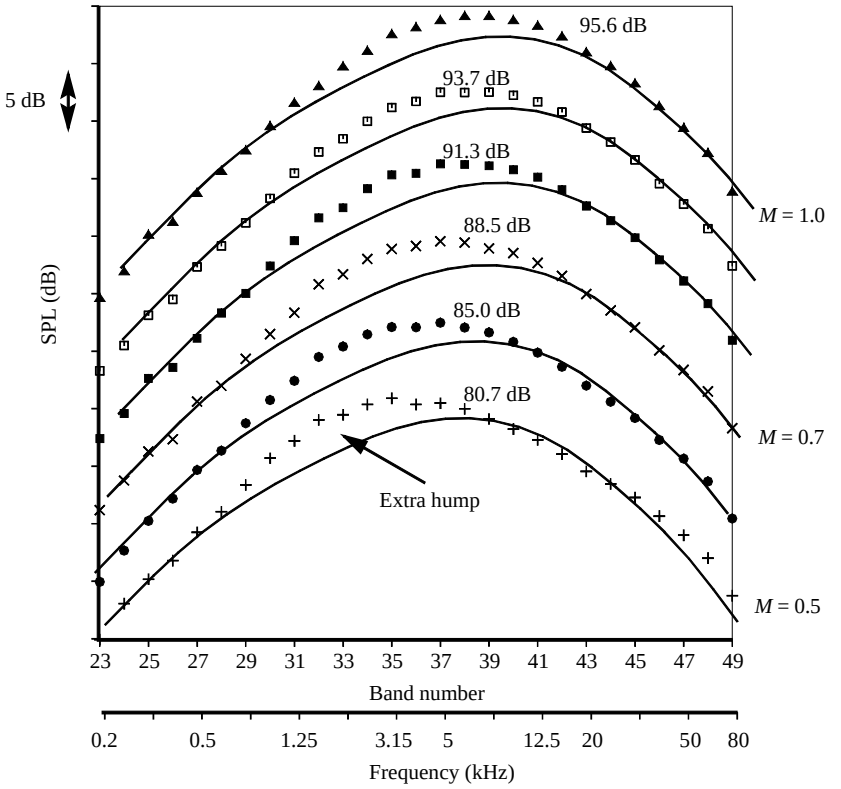

FIGURE 14. Comparison of measured spectra with fine-scale similarity spectrum. $T_t/T_a = 3.2$, angle = 90°, $D = 1.5$ in. +, $M = 0.5$; ●, 0.6; ×, 0.7; ■, 0.8; □, 0.9; ▲, 1.0.

cause more noise. Recently, Tam & Ganesan (2003) suggested that at very high temperatures, these fluctuations could produce more turbulence, leading to higher mixing in the jet plume. This higher mixing in turn could potentially generate more mixing noise. Based on this premise, Tam & Ganesan (2003) developed an additional term to capture this effect in the flow field computation. With the modified CFD results, which serve as the input for the model of Tam & Auriault (1999), they demonstrated much better agreement with the highly heated supersonic jet data of Seiner *et al.* (1992). However, this approach must be validated against the current subsonic data.

4.3. *Spectral characteristics at angles close to the jet exhaust axis*

Some interesting findings on cold jets are first presented; the effects of jet temperature on spectra are then discussed. It is now accepted widely that the noise generated by the instability waves/large-scale structures of high-speed jets is dominant, especially in the peak radiation sector, at angles close to the jet axis. For supersonic jets, and subsonic jets at high temperatures, the large-scale structures propagate downstream at supersonic speeds relative to the ambient speed of sound. As such, these structures are efficient generators of noise. However, for subsonic jets, especially at low and moderate temperatures, the large turbulence structures propagate downstream at subsonic speeds relative to the ambient speed of sound. For these low-speed jets, the noise from these large structures has been thought to be unimportant. The measured spectra from unheated jets at two Mach numbers of 0.4 and 0.5, and comparisons

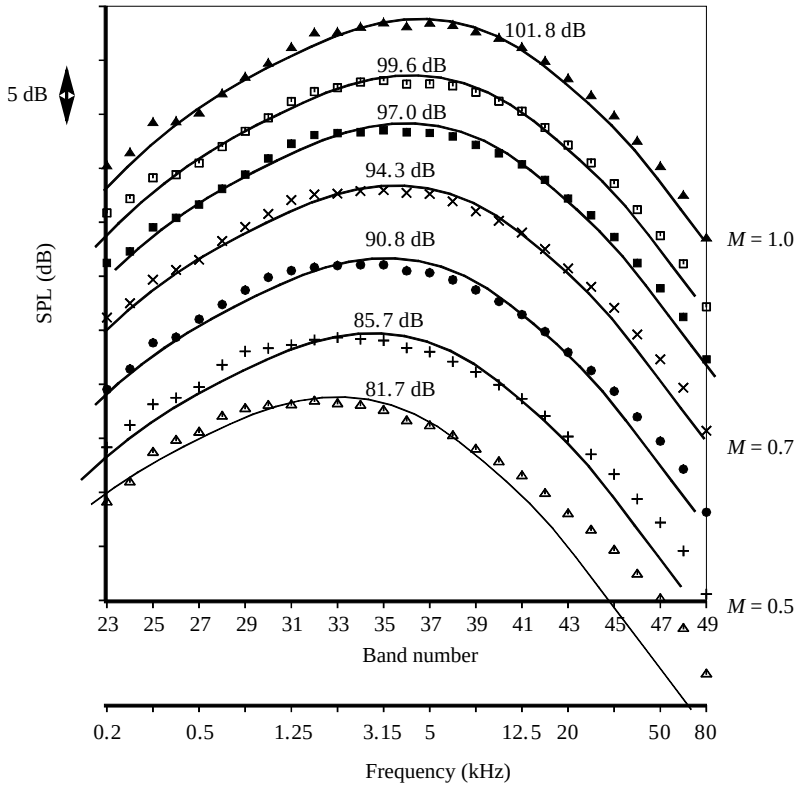

FIGURE 15. Comparison of measured spectra with FSS spectrum. $T_t/T_a = 3.2$, angle = 90°, $D = 3.46$ in.; △, $M = 0.4$; +, 0.5; ●, 0.6; ×, 0.7; ■, 0.8; □, 0.9; ▲, 1.0.

with the similarity spectra are presented in figure 18. Spectra at two angles of 90° and 155°, corrected to standard day atmospheric conditions and to a polar distance of 20 ft (6.096 m) are shown. The measured spectra at 90° are characterized well by the FSS spectrum. However, the spectral shapes at 155° are very different and are seen to fit the large-scale-similarity (LSS) spectrum. Recall that the shape of the LSS spectrum was extracted from supersonic spectra. (There are some tones at the low frequencies caused by reflections from the exhaust collector, since the microphones at very large angles are close to the collector given the microphone arrangement). Comparison of the measured spectra at 160°, from unheated jets at several Mach numbers, with the LSS spectrum is shown in figure 19. There is excellent agreement even at the lower Mach numbers of 0.4 and 0.5. The reason for the mismatch at the highest frequencies is atmospheric attenuation effects, as explained in Viswanathan (2002). The peak frequency, denoted by the dashed line, is seen to be independent of jet velocity. Lush (1971) first noted this characteristic.

There are two schools of thought on the reason for the observed change in spectral shape at large aft angles. The trends seen in figure 18 were also noted in the early measurements of Lush (1971) and Ahuja (1973). In the traditional view, the observed increase in level at low frequencies is attributed to amplification caused by eddy convection, while the large reduction in amplitude at high frequencies is thought to be caused by mean-flow/acoustic interaction and refraction. However, the importance of the large-scale-structures/instability waves in noise generation is not recognized.

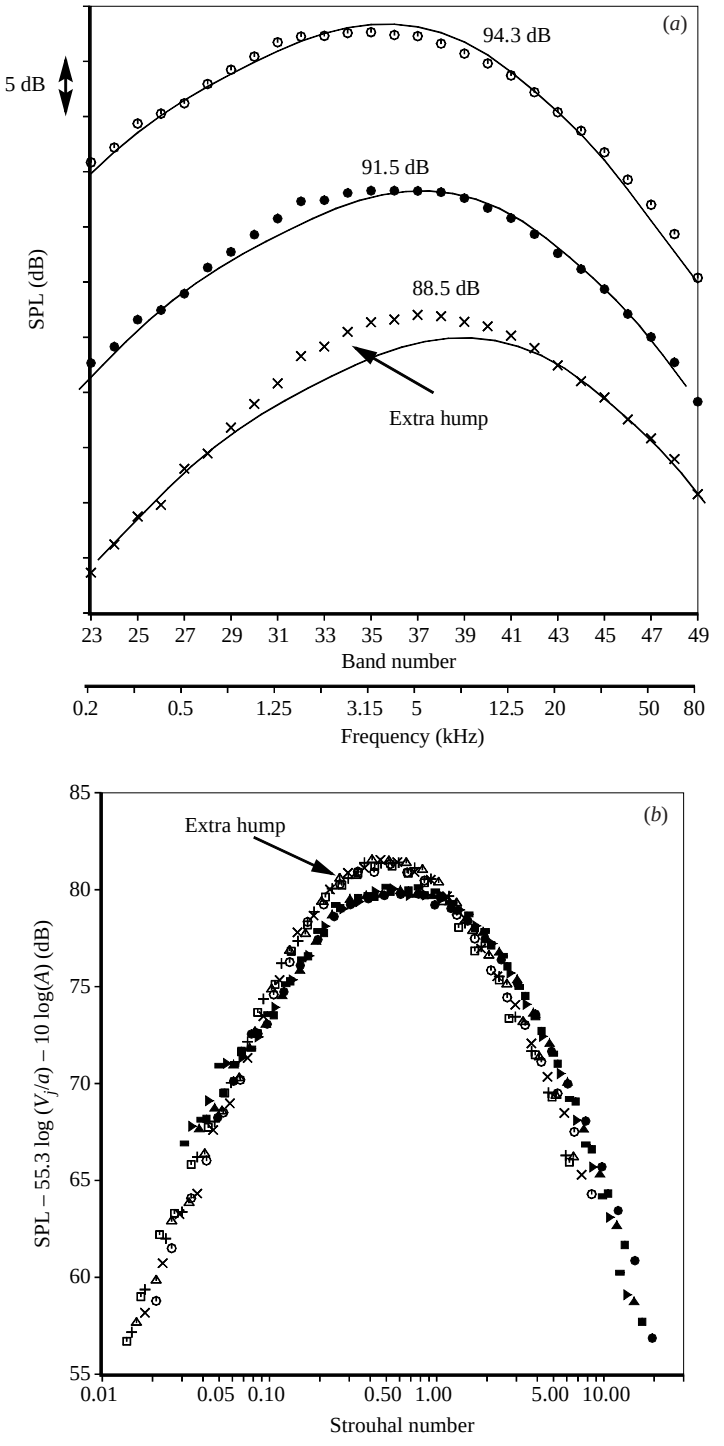

FIGURE 16. (*a*) Comparison of measured spectra with fine-scale similarity spectrum. $M = 0.7$, $T_t/T_a = 3.2$, angle $= 90°$. ×, $D = 1.5$ in.; ●, 2.45 in.; ○, 3.46 in. (*b*) Comparison of normalized spectra. $T_t/T_a = 3.2$, angle $= 90°$. Open symbols: $D = 1.5$ in.; closed symbols $D = 3.46$ in.

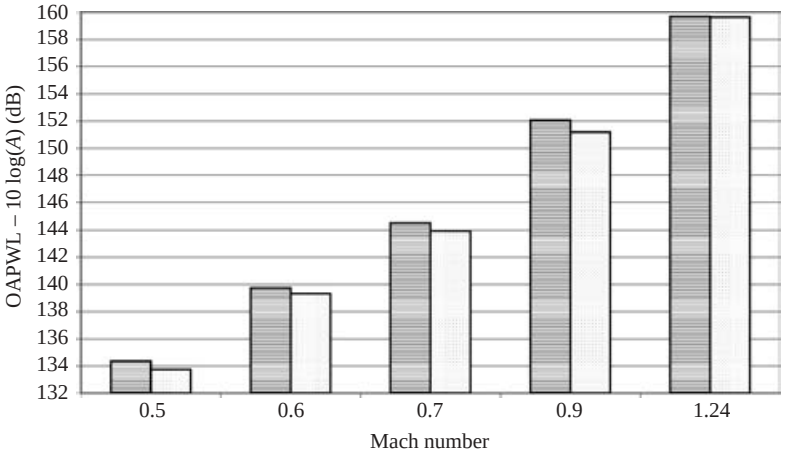

FIGURE 17. Comparison of overall power at different Mach numbers. $T_t/T_a = 3.2$. Grey: $D = 1.5$ in.; dots: $D = 2.45$ in.

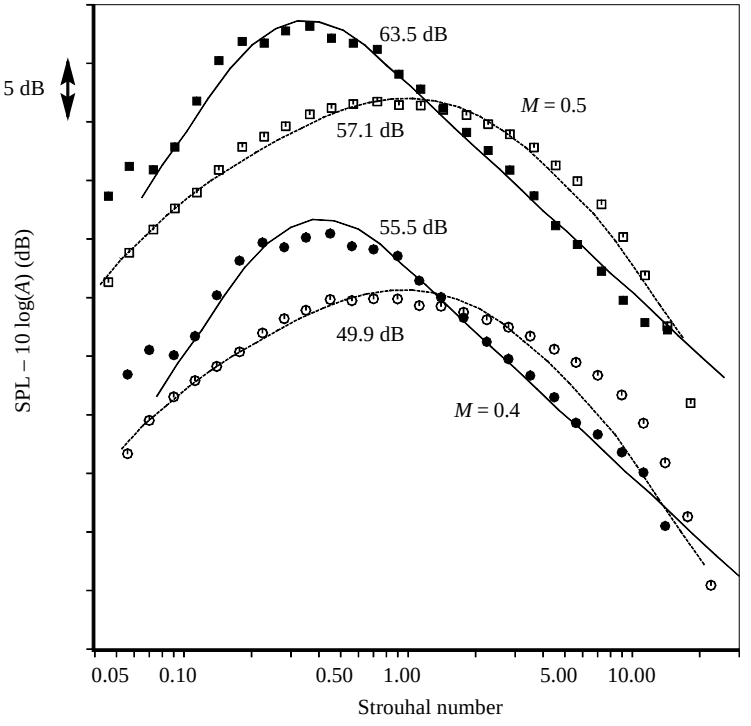

FIGURE 18. Comparison of measured spectra with similarity spectra. Unheated jets. $D = 1.5$ in. Solid line: large-scale similarity spectrum; dashed line: fine-scale similarity spectrum. ○, $M = 0.4$, 90°; ●, 0.4, 155°; □, 0.5, 90°; ■, 0.5, 155°.

This view is not universally accepted and there is no consensus on the reason for the observed change in spectral shape as yet.

The second point of view, advanced by Tam (1991), among others, is that the noise radiation in the aft directions is generated directly by the large-scale structures. As in Tam *et al.* (1996), the noise radiated by the fine-scale turbulence has uniform

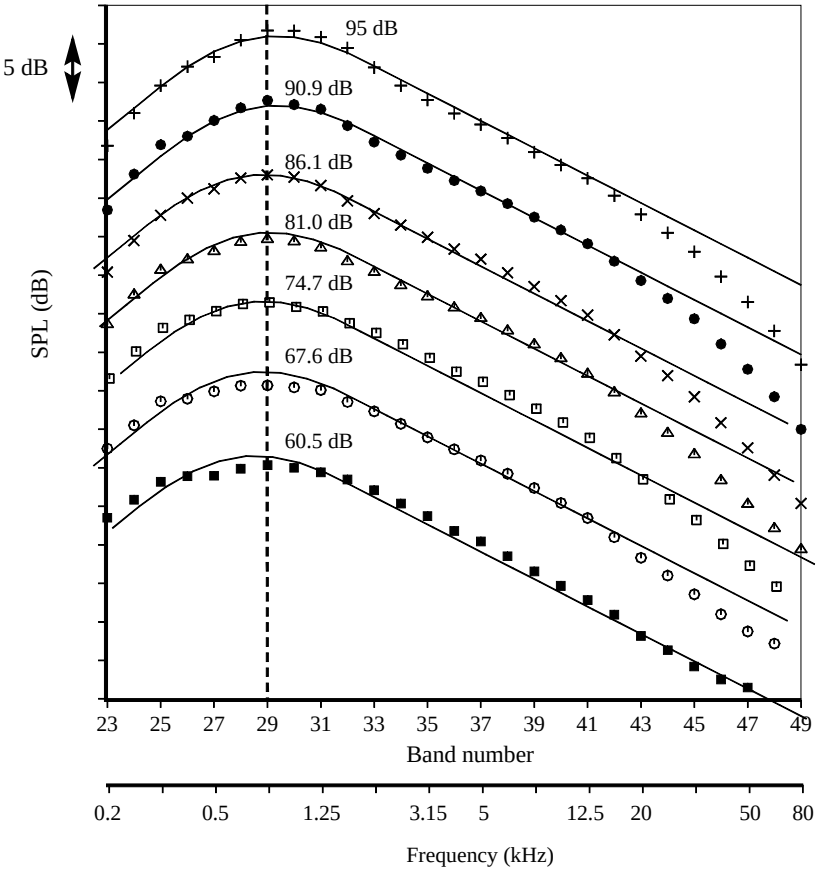

FIGURE 19. Comparison of measured spectra with large-scale similarity spectrum. Unheated jets. $D = 2.45$ in., angle $= 160°$. ■, $M = 0.4$; ○, 0.5; □, 0.6; △, 0.7; ×, 0.8; ●, 0.9; +, 1.0.

directivity. Hence, the noise increase seen at large aft angles is not due to the fine-scale component. This argument, coupled with the observation that the spectral shape changes to that of the LSS spectrum, suggests that the contribution of the noise generated by the large-scale structures is indeed important at large aft angles even for subsonic jets. What possible mechanism then would lead to this noise generation? The physical process by which large-scale structures generate noise in high-speed jets has been explained using the wavy-wall analogy. Supersonic flow over a wavy wall produces intense directional radiation of noise, the so-called Mach wave radiation. For a comprehensive treatment of this noise generation mechanism, as applied to high-speed flows, see Tam (1991). However, the situation is very different here (figures 18 and 19): the Mach numbers are very low in these cases. If we assume a convective speed for the large-scale structures to be $\approx$70% of the jet velocity, then the velocity of these structures relative to the ambient speed of sound (V/a, where a is the ambient speed of sound) is $\approx$0.3, for the unheated jet at a Mach number of 0.4. Turbulence structures travelling at this very low relative velocity cannot generate acoustic waves. Therefore, a possible mechanism could be due to the rapid and catastrophic decay or destruction of the instability waves. It is well known that a modulation in amplitude of an instability wave at a fixed frequency leads to

a broadening of the wavenumber spectrum, with some low-wavenumber components with potentially supersonic phase speeds relative to the ambient speed of sound, see Tam & Burton (1984). This part of the spectrum with supersonic speeds could generate noise. For the low Mach number jet, the amplitude modulation has to be severe and drastic enough to generate these supersonic components. Instability waves at low Strouhal numbers evolve more gradually closer to the nozzle exit than waves at higher Strouhal numbers, and attain their peak amplitudes close to the end of the potential core. Furthermore, the instability waves of subsonic jets have higher growth rates than those of high-speed jets. Just downstream of the end of the potential core, where the shear layer disappears, there is no mechanism for the instability waves to extract energy from the mean flow and hence they become damped. Given the frequency content of the spectra and the spectral shape that corresponds to that of the LSS, it is entirely plausible that the rapid decay of the instability waves due to nonlinear mechanisms, just downstream of the potential core, could be the physical mechanism responsible for the generation of noise. Indeed, the well-established fact that the peak noise of the large-scale structures is generated near the end of the potential core for high-speed jets lends more credence to the above supposition.

Recently, Panda & Seasholtz (2002) investigated the axial variation of density fluctuations along both the jet centreline and the peripheral shear layer at various jet Mach numbers. The correlations of these fluctuations with a far-field microphone located at an angle close to the jet axis exhibited some interesting trends. At supersonic convective Mach numbers, significant correlation was measured from the peripheral shear layer, while there was no such correlation at subsonic convective Mach numbers. However, significant correlations at low Strouhal numbers were observed with the fluctuations along the jet centreline just downstream of the potential core, for unheated jets over a wide range of Mach numbers from 0.6 to 1.8. These observations indicate that the region downstream of the potential core is a low-frequency sound source, with a noise generation mechanism very different from the Mach wave emission associated with supersonic convective velocities. The measurements by Panda & Seasholtz (2002) provide tantalizing evidence that supports the noise generation mechanism proposed here. However, there is no definitive and widely accepted mechanism for the change in spectral shape at large aft angles and this issue still remains unresolved.

A comparison of the measured spectra at 155° from a Mach 0.7 jet at various temperature ratios with the LSS spectrum is shown in figure 20. Attention is drawn to several features in this figure. First, the spectral shape becomes more peaked as the jet is heated, as denoted by the mismatch between the data and the LSS spectrum. This is so even for a temperature ratio of 1.8; the corresponding Reynolds number is 642 600 and hence this phenomenon is not an effect attributable to low Reynolds number (the value of a critical Reynolds number is discussed in a later section). This characteristic is observed at other Mach numbers as well, at large aft angles. Secondly, the peak frequency of the one-third-octave spectra shifts to higher values, more noticeable in the two highly heated cases (this trend has been confirmed from narrowband data as well). The values of (V_j/a), also referred to as the acoustic Mach number, are 1.11 and 1.2, respectively, for these two cases. An examination of the spectra at various Mach numbers and temperature ratios indicates that the peak spectral frequency at large aft angles of 155° and 160° remains unchanged and is independent of jet velocity as long as the acoustic Mach number is less than unity. This trend was seen in figure 19 for cold jets; similar behaviour is observed for hot jets with subsonic acoustic Mach numbers.

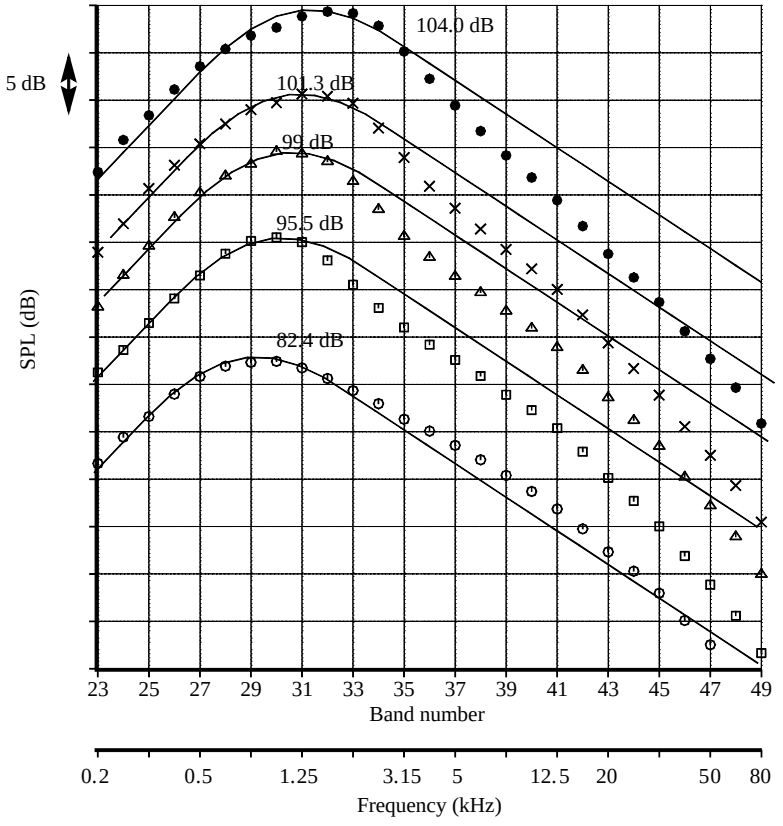

FIGURE 20. Comparison of measured spectra with large-scale similarity spectrum. $M = 0.7$, angle = 155°. ○, $T_t/T_a = 1.0$; □, 1.8; △, 2.2; ×, 2.7; ●, 3.2.

In figure 21, the measured spectra at various Mach numbers and at a temperature ratio of 3.2 are shown. Contrast this figure with figure 19. Though it is tempting to conclude that the peak frequency increases with jet velocity, an examination of narrowband (23.4 Hz) spectra in figure 22 for selected Mach numbers (of 0.4, 0.6, 0.8 and 1.0) indicates that it is not so clear-cut. There is a very large broadening of the peak, especially at higher Mach numbers. The spectrum from an unheated jet ($M = 0.5$) is also included for perspective. An attempt was made to identify the peak frequency from the narrowband spectra. However, because of the flatness at the peak and the little blips in the spectra, no consistent peak (that would perhaps follow a Strouhal number scaling) could be readily identified. Also shown in figure 22 is a comparison with the LSS spectrum for the heated cases. It is seen that there is a significant increase in the spectral level at the lower frequencies. This increase is observed in the spectra at other large aft angles and for other higher temperature cases as well.

4.4. *Velocity dependence of sound power and the consequence of rig noise*

The variation of the power radiated by unheated and heated subsonic jets is examined next. Jets at six Mach numbers of 0.5, 0.6, 0.7, 0.8, 0.9 and 1.0 and at five different temperature ratios of 1.0, 1.8, 2.2, 2.7 and 3.2 are considered in the following analyses. The nozzle diameter is 2.45 in. or larger, to avoid Reynolds number effects. In a later

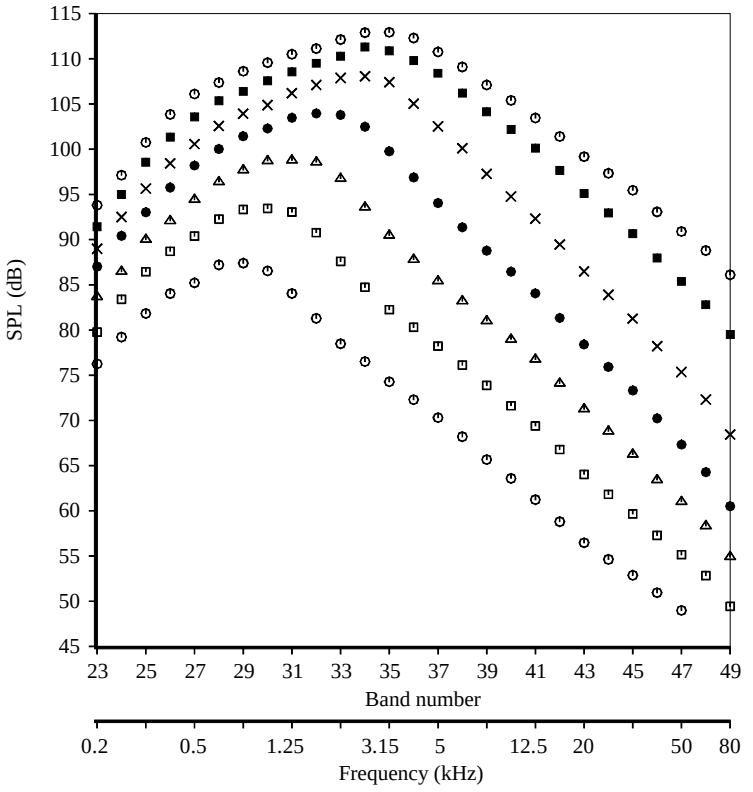

FIGURE 21. Measured spectra. $T_t/T_a = 3.2$, $D = 2.45$ in., angle $= 155°$. ○, $M = 0.4$; □, 0.5; △, 0.6; ●, 0.7; ×, 0.8; ■, 0.9; ○, 1.0.

section, the value for a critical Reynolds number is investigated. Again, the power levels and overall sound pressure levels have been computed per unit nozzle area. The variation of overall power level (OAPWL) with acoustic Mach number is shown in figure 23. Also shown is a line representing a V^8 variation. At first look, all the points seem to follow the eighth-power law. Let us take a closer look and isolate the temperature effect by grouping the points by temperature ratio. Figure 24 shows the same plot, with the curves spaced apart, and a least-square fit through each group. As can be seen, the value of the velocity exponent decreases with increasing temperature, from a value of 8.74 for unheated jets to a value of 7.98 for heated jets at a temperature ratio of 3.2. Note that the value of the exponent is close to 8 for the highly heated cases. In figure 23, two other values at Mach numbers of 0.3 and 0.4 (unheated) were included, denoted by the open squares. At these low Mach numbers, rig noise becomes an issue and the value of the velocity exponent obtained with these two values included with the other six, yields a value of 8.41 (down from 8.74) for the unheated cases. It is clear that contamination by rig noise, which is a big factor at low Mach numbers, could influence the value of the velocity exponent as shown in the above example. Similarly, inclusion of heated jet data subject to the Reynolds number effects (see figure 14) could lead to a different value for the velocity exponent. It is noted here for reference that for $T_t/T_a = 3.2$, the value of the exponent with the inclusion of lower Mach numbers of 0.3 and 0.4, and a smaller nozzle ($D = 1.5$ in.) is 7.32, as opposed to 7.98 seen in figure 24.

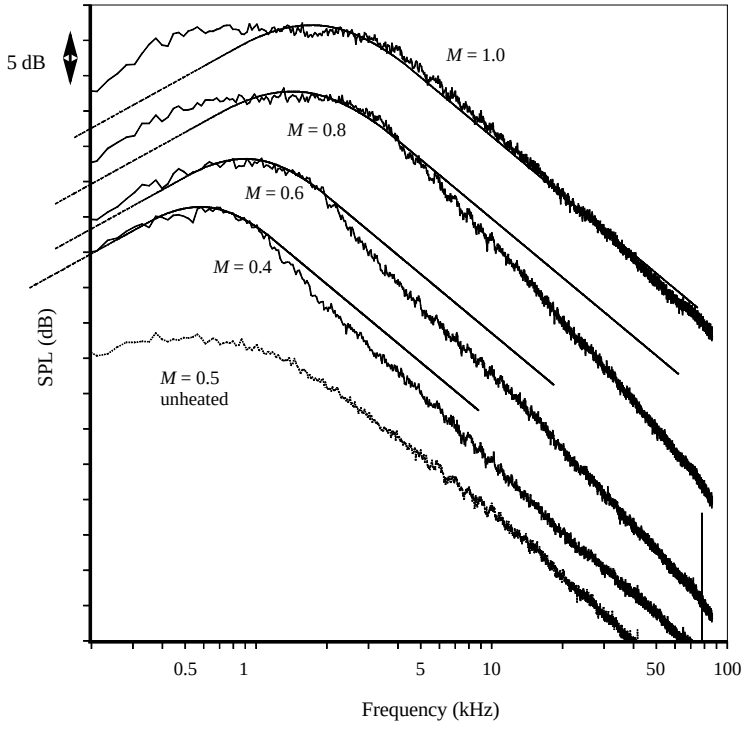

FIGURE 22. Measured spectra and comparison with large-scale similarity spectrum (dashed line). $T_t/T_a = 3.2$, $D = 2.45$ in., angle $= 155°$.

The following exercise is carried out to ascertain that there is no discernible V^6 trend in the data from heated jets over the uncontaminated velocity range. First, the OAPWL at the highest two temperature ratios is normalized with the subtraction of $80\log(V_j/a)$, and the results shown with an expanded ordinate axis in figure 25. A least-square fit for each set of data is also shown in the figure. If there were only an eighth-power dependence, then the curve fits would be parallel to the x-axis; if there were a sixth-power dependence, these lines would slope sharply downward to the right. The slopes of these lines, i.e. the values of the exponents (relative to 8), are 0.028 and -0.013, respectively, for the two temperature ratios of 2.7 and 3.2. Note that the individual values are within ± 0.5 dB from the curve fit, showing the slight scatter in the data. The variations of the power spectra for the different Mach numbers at the highest temperature ratio of 3.2 are shown in figure 26. When the spectra are normalized as in figure 25, there is good collapse of the spectra as seen in figure 27. Two observations about this figure are in order. The spectral peaks at the higher Mach numbers are broader; this trend is expected given the broadening of the sound pressure level spectra in the peak noise radiation directions when the value of (V_j/a) exceeds unity, as noted in figure 21 (one should contrast figures 21 and 22 with figure 19). Furthermore, there is an increase of $\sim$16 dB in OASPL in the peak radiation angles compared with the noise level at 90° for the jet at $M = 1.0$. Thus, any broadening of the spectra in the peak angles would have a large influence on the shape of the power spectrum. At a Strouhal number of $\sim$0.5 in figure 27, the power level for the jet at a Mach number of 1.0 ($V_j/a = 1.64$) is $\sim$3 dB higher than that for the jet at $M = 0.5$ and 0.6 ($V_j/a = 0.88$ and 1.05). The second region of discrepancy

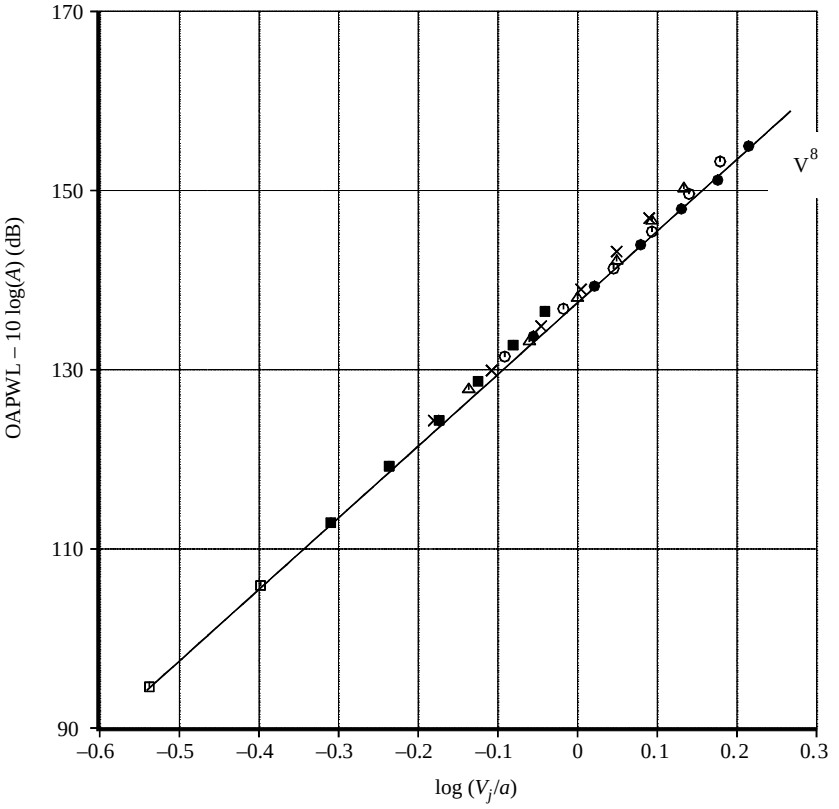

FIGURE 23. Variation of OAPWL with jet velocity, $D = 2.45$ in. Solid line: V^8. □, ■, $T_t/T_a = 1.0$; ×, 1.8; △, 2.2; ○, 2.7; ●, 3.2.

occurs at the very high frequencies. At a Strouhal number of 10.0, the power level for the jet at $M = 0.5$ has the highest value. This behaviour is attributable to the influence of the rig noise being stronger at lower Mach numbers, as suggested by figure 15. The rest of the curves collapse to within 2 dB over a large Strouhal number range of ~1.5 to ~10.0, with a tighter collapse in the range of ~3.0 to ~7.0. However, the eighth-power dependence is strongest at the lower frequencies to the left of the spectral peak.

In addition to the spectral comparisons shown in figures 9–16, quantitative comparisons have been provided in figures 24–27. It is evident that at no jet temperature is a V^6 dependence detected. Proponents of dipoles have maintained that the overall power radiated by hot jets depicts a sixth-power velocity dependence; see for example Lilley (1996). The supposed sixth-power dependence has also been used in the past by many researchers to justify the existence of dipoles. A closer scrutiny reveals that many subscribers to this school of thought cite the same two sets of data, that of Tanna *et al.* (1975) and Hoch *et al.* (1973), to support their contention. Let us investigate how this view could have prevailed for so long.

Till recently, there was no sure way of assessing if the measured jet noise data were free from contamination by extraneous sources. For example, the spectra shown in figure 13 at the lower two temperature ratios of 1.0 and 1.8 would have been considered to be of good quality a few years ago, since the contamination at the higher frequencies is not very obvious. Previously, an eighth-power dependence of

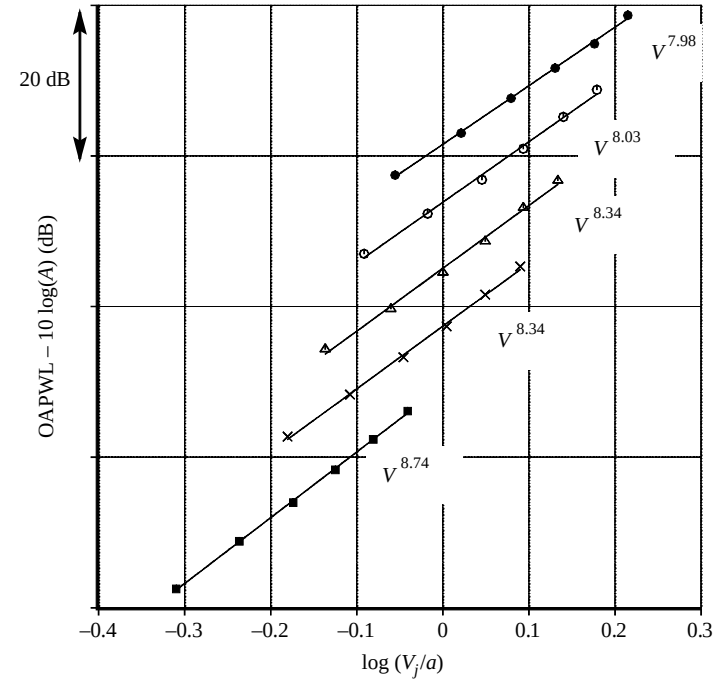

FIGURE 24. Variation of OAPWL with jet velocity, $D = 2.45$ in.
■, $T_t/T_a = 1.0$; ×, 1.8; △, 2.2; ○, 2.7; ●, 3.2.

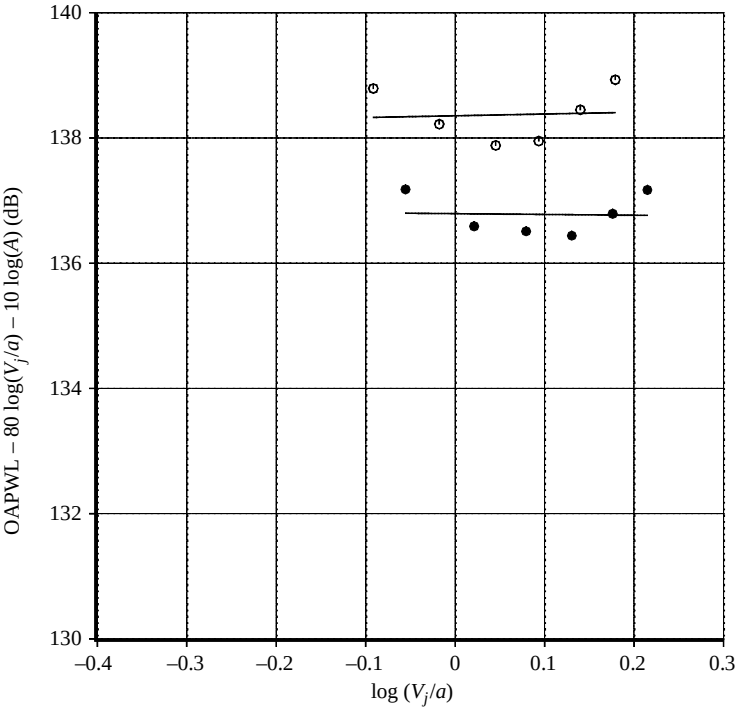

FIGURE 25. Variation of normalized OAPWL with jet velocity, $D = 2.45$ in.
Lines: least-square fit. ○, $T_t/T_a = 2.7$; ●, 3.2.

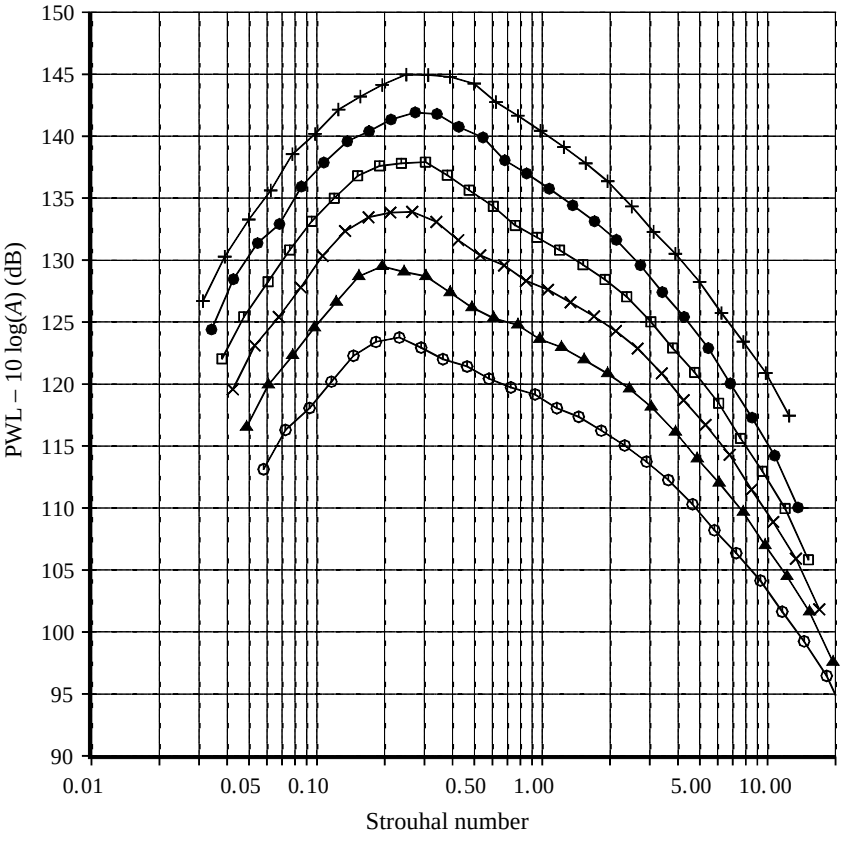

FIGURE 26. Variation of power spectra with jet velocity, $D = 3.46$ in. $T_t/T_a = 3.2$. ○, $M = 0.5$; ▲, 0.6; ×, 0.7; □, 0.8; ●, 0.9; +, 1.0.

intensity at a particular angle or OAPWL was thought to be adequate to establish good quality of data. Bushell (1971) and Ahuja & Bushell (1973) adopted such a practice. However, the summation of amplitudes over the entire frequency range for obtaining intensity or OASPL hides a multitude of problems in the spectra, as shown below. It is emphasized once again that good quality spectra at all angles and all frequencies are vital, especially for aircraft applications. A novel method for determining the qualitative goodness of measured spectra, using the universal similarity shape, was introduced and demonstrated by Viswanathan (2003). This method permits easy identification of rig noise, the affected frequencies, and the magnitude of contamination for any jet operating condition. Several examples were shown in Viswanathan (2003), and it was emphasized that when the spectra are smooth it is difficult to identify potential problems, even if the magnitude of the contamination is ~10 dB or more. Quantitative goodness of data was established through comparison with data obtained with a blow-down tunnel. In some of these examples, discrepancies of 4 or 5 dB across the entire spectrum were noted before suitable rig modifications eliminated the problems with rig-generated noise. Also, the magnitude of the contamination was shown to be highly dependent on the jet Mach number and temperature. Similar trends are observed in the data from NGTE and Tanna *et al.* (1975) and Tanna (1977) as seen in figures 3–5. If one were to compute, say the OASPL at 90°, with the contaminated data shown in Viswanathan (2003), the levels

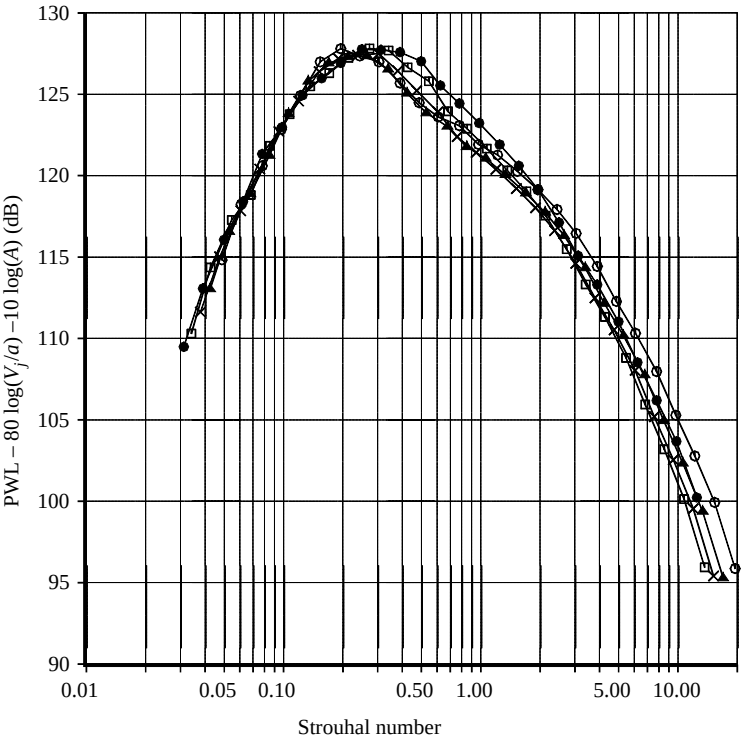

FIGURE 27. Variation of normalized power spectra with jet velocity, $D = 3.46$ in. $T_t/T_a = 3.2$. ○, $M = 0.5$; ▲, 0.6; ×, 0.8; □, 0.9; ●, 1.0.

would be higher by ∼5 dB or more at lower jet velocities. As discussed in figures 23 and 24, inclusion of such bad data would decrease the value of the velocity exponent significantly, potentially reaching a value of 6.

We now demonstrate that this is not speculation but a distinct possibility, with the following discussion. It was mentioned that many of the observations of the noise characteristics and the development of a prediction method for jet noise by Morfey *et al.* (1978) was based on data from Tanna and NGTE. There have also been many claims about the excellent quality of these data sets. To verify these claims, data were acquired at several test points from the test matrix given in Tanna *et al.* (1975) both for heated and unheated jets and in Ahuja (1973). It should be kept in mind that much of the data from hot jets by Hoch *et al.* (1973) were also acquired at NGTE around the same time period. Spectral comparisons at 90°, with data from these two facilities were presented in figures 3–5. Note that the Mach numbers were fairly high: 0.55 and 0.95 for the NGTE data and 0.62, 0.74 and 0.98 for Tanna's data. The values of (V_j/a) span a range of 0.53 to 0.9 for these Mach numbers. Let us re-examine figures 3–5. Spectral variations are plotted as a function of raw frequencies in figures 3 and 4 rather than Strouhal numbers for a specific purpose. There is reasonable agreement at the lowest frequencies for the NGTE data while there is very good agreement between the two sets of data at lower frequencies, to the left of the peak frequency for Tanna's data. However, at higher frequencies (>6000 Hz), the data from Tanna start to diverge and the magnitude of the discrepancy increases with increasing frequency. There is a ∼5 dB increase above a frequency of ∼13 000 Hz in Tanna's data. This

trend is more glaring in the NGTE data. Evidently, there is rig noise contamination at the higher frequencies. It is worth noting that the discrepancy in OASPL for the three cases of Tanna is only ~1.7 dB, even though the high-frequency portion of the spectra are significantly off. When scaled to engine-scale frequencies, the high-frequency portion of the spectra from model-scale nozzles become important as they fall in the range of frequencies with maximum annoyance penalty. Therefore, the use of gross quantities such as OASPL or OAPWL for assessing the quality of data could be highly misleading and hence must be avoided.

The spectral content of an internal source of rig noise is usually a function of raw frequency; i.e. a high tone at 20 000 Hz, for example, stays at this frequency regardless of the jet velocity and nozzle size. Therefore, examination of spectra in terms of raw frequency aids in the easy identification of rig noise problems and the affected frequencies. The contamination at the higher frequencies is not restricted to data from just these two rigs. Similar problems at higher frequencies were identified in the spectra obtained at three other jet facilities and reported in Viswanathan (2003). In fact, the rig noise characteristics are very similar to those of facility 3 (see the above reference), where a high-frequency problem was noted at all frequencies above ~10 000 Hz. Comparisons for heated jets are not presented for the following reason. The effects of Reynolds number on spectral shapes of hot jets have been established above; the spectra from a nozzle of 1.5 in. diameter are subjected to these effects, while those from a nozzle of 2.45 in. diameter are not. Since the diameter of the nozzle used (2.0 in.) is in the middle, a proper comparison is not possible. Just as seen with the heated spectra at low Mach numbers in the current data (see figure 13, for example), the influence of the rig noise decreases as the jet temperature is increased, in the data of Tanna.

Direct comparison with current data indicates that the data from these rigs are subject to contamination by extraneous sources of noise over a wide range of higher frequencies, contrary to the claims of clean data. In addition, Tanna's data exhibit the effects of low Reynolds number identified here (as seen in figure 10). The hot jet data of Hoch *et al.* (1973) from NGTE were also obtained with a smaller nozzle ($D = 1.78$ in.). As pointed out, the Mach numbers (or V_j/a) are fairly high in these comparisons. Experience has shown that the magnitude of contamination is more pronounced at lower jet velocities. Spectra were acquired down to very low velocity ratios of 0.44 at NGTE, 0.35 by Tanna and 0.25 at ISVR, see figure 20 in Morfey *et al.* (1978). The presence of dipoles was detected at these low velocity ratios. Given the magnitude of the contamination at the higher (V_j/a) shown here, one should treat data at very low jet velocities with caution. Therefore, it is fair to conclude that the measurements at the low velocities could represent rig noise and not real jet noise.

To further emphasize this point, we now present data acquired at very low jet velocities at a temperature ratio of 3.2. The variation of OAPWL is shown in figure 28. The jet Mach numbers for the four lower points are 0.18, 0.22, 0.25 and 0.28, corresponding to (V_j/a) of 0.32, 0.39, 0.44 and 0.49, respectively. The upper three points are at slightly higher Mach numbers of 0.4, 0.5 and 0.6. These seven points yield a velocity exponent for OAPWL of 5.9. The corresponding value for OASPL at 90° is 5.2. When all the data points at this temperature ratio (including $M = 0.7$ to 1.0) are used, the value of the exponent for OAPWL is 6.3. When we examine the spectra for the seven Mach numbers at two angles of 140° and 90° in figures 29(*a*) and 29(*b*), respectively, the reason for the reduction in the velocity exponent from 7.98 to ~6.0 becomes clear. The spectra at the four low Mach numbers (or V_j/a) have been contaminated by rig noise. This is quite obvious in figure 29(*b*), where

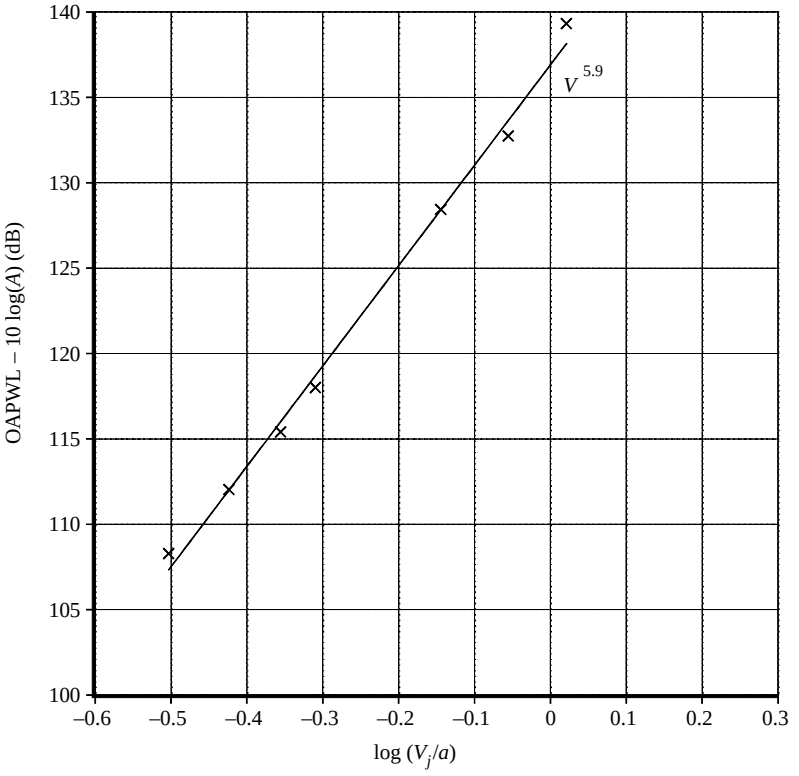

FIGURE 28. Variation of OAPWL with jet velocity at low (V_j/a). $T_t/T_a = 3.2$. Solid line: least-square curve fit.

the low-frequency levels could be higher by $\sim$20 dB. This level of contamination is not unexpected given the impact of the rig noise noted in earlier figures and in Viswanathan (2003). However, it is crucial to recognize this problem and interpret the result in figure 28 correctly as being due to rig noise and not due to the appearance of additional noise sources of the dipole type. It is recognized that a few uncertainties remain. It would be valuable to obtain clean spectra at very low (V_j/a), while still maintaining a high value of Reynolds number with a large enough nozzle. This is not an easy task as can be appreciated by the complexities discussed here.

It has been shown here, with concrete examples, how the inclusion of contaminated data could decrease the value of the velocity exponent, since the impact of rig noise is greatest at lower jet velocities. Since Tanna *et al.* (1975) used convergent–divergent nozzles with design Mach numbers of 1.4, 1.7 and 2.0, they were able to acquire data at high velocities. The supersonic points in the power–velocity plots, which are usually not subject to rig noise, or only minimally, would anchor the curves at the high end while the contaminated data at lower velocities would drive the values of the velocity exponent lower. Regardless, the value of the velocity exponent by itself is just one indicator. The current data directly contradict the proposed multi-pole nature of the sources of jet noise, based on the justification of change in spectral shape due to heating and sixth-power velocity dependence. Serious doubts have been raised about the experimental evidence used to support the contention that an additional dipole component is important for hot jets. Given the new finding, a re-examination of the

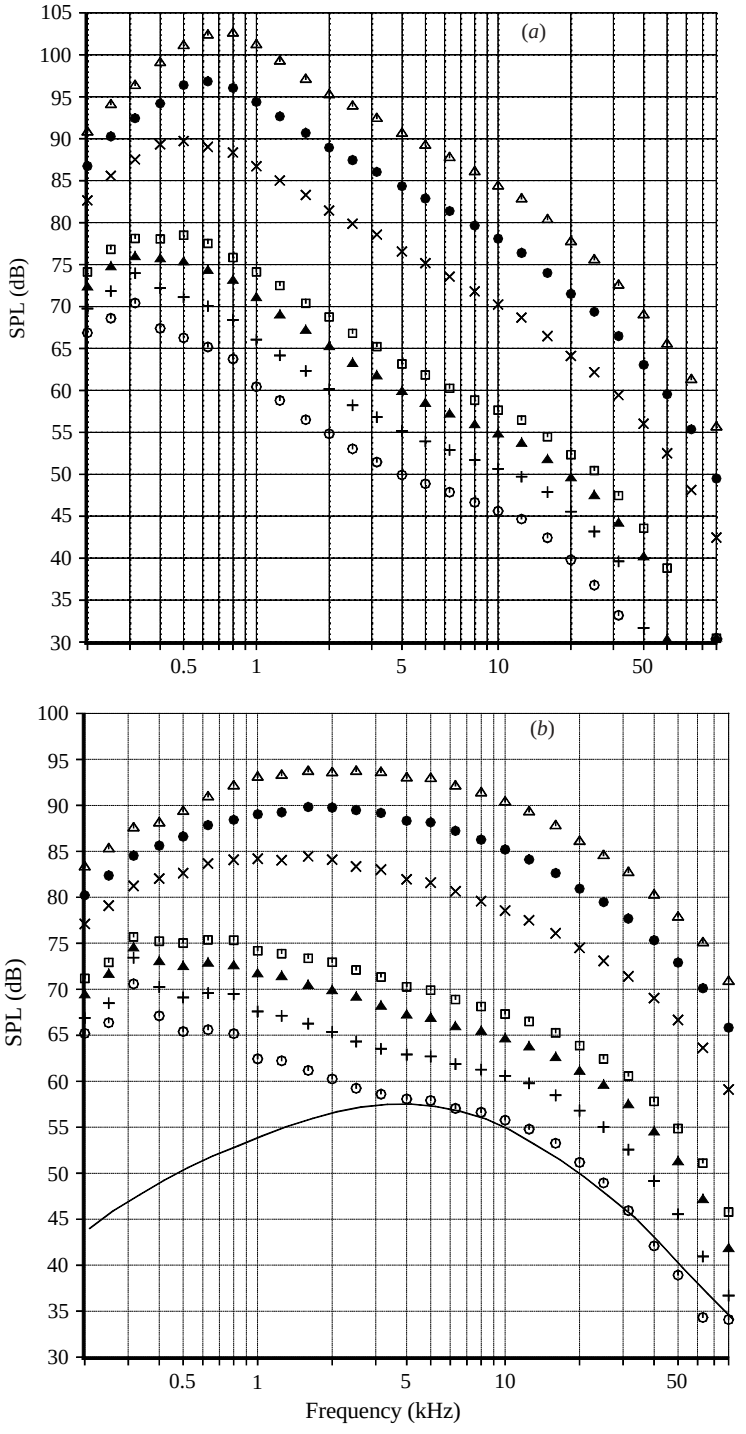

FIGURE 29. Measured spectra at low (V_j/a), $T_t/T_a = 3.2$; (*a*) angle = 140°, (*b*) 90°, ○, $M = 0.18$; +, 0.22; ▲, 0.25; □, 0.28; ×, 0.4; ●, 0.5; △, 0.6. Line in (*b*) is FSS.

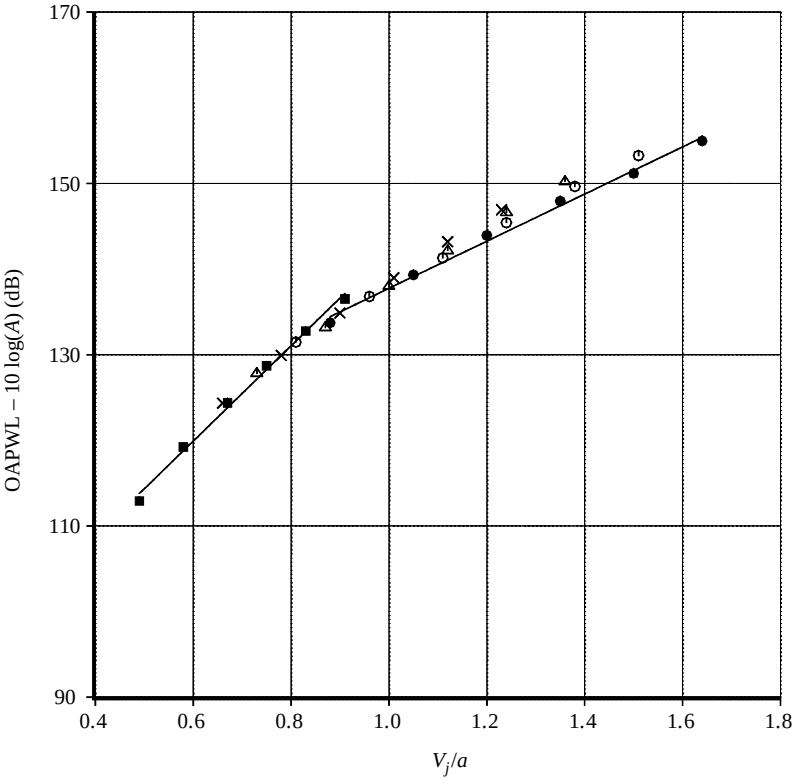

FIGURE 30. Variation of OAPWL with jet velocity, $D = 2.45$ in.; ■, $T_t/T_a = 1.0$; ×, 1.8; △, 2.2; ○, 2.7; ●, 3.2.

use of these source terms in many theoretical jet noise prediction methods is perhaps warranted. Two recent studies are pertinent when we discuss the nature of the sources of jet noise. Morris & Farassat (2002) showed that the interpretation of source terms and their meaning are largely based on how the governing equations are cast. Goldstein (2002) derived a different set of linearized inhomogeneous Euler (LIE) equations that produced monopoles and quadrupoles as the source terms. Goldstein cautions, "It is important to note that this does not imply that the LIE equations, or for that matter any other 'acoustic analogy' equations can provide an unambiguous identification of the sources". The temperature/density fluctuations due to heating could indeed lead to increased noise levels; the suggestion by Tam & Ganesan (2003) for a possible mechanism warrants further investigation. It is noteworthy that Tam chose to incorporate the effect of density fluctuations only in the flow field computations. The theory for noise generation and the prediction method were unaltered. This approach marks a welcome departure from the common practice of adding more 'source terms' in the acoustic models when poor agreement with data is obtained.

4.5. *Noise of jets at constant velocity – the density effect*

Next, the issue of the noise of jets at constant velocity, the so-called density effect, is examined. With a suitable combination of NPR and temperature, one could attain a desired jet velocity. First we re-examine the variation of the radiated overall power with velocity, in figure 30. For the sake of clarity, a linear scale is used on the

x-axis. Least-square curve fits for the two extreme temperature cases, $T_t/T_a = 1.0$ and 3.2, are also shown. The slopes of these two curves suggest that, at an acoustic Mach number of ~0.8, the two curves could intersect. Also, this figure suggests that there is a small velocity range in which the power radiated by jets at different temperatures would be more or less the same. Hoch *et al.* (1973) and Tanna *et al.* (1975) quoted a value of 0.73 from their measurements. However, as seen in figure 30, pinpointing a single value would be very difficult. Furthermore, the trends allow for the possibility that at lower relative velocities, a heated jet could produce more noise than a cold jet at fixed velocity, while the reverse is true in the higher velocity range.

To answer the issues associated with density variation, measurements were taken at six values of (V_j/a) of 0.53, 0.62, 0.73, 0.8, 0.9 and 1.2. The corresponding jet velocities are 600 ft s^{-1} (183 m s^{-1}), 700 ft s^{-1} (213 m s^{-1}), 820 ft s^{-1} (250 m s^{-1}), 900 ft s^{-1} (274 m s^{-1}), 1010 ft s^{-1} (308 m s^{-1}) and 1350 ft s^{-1} (412 m s^{-1}), respectively. Since convergent nozzles have been used, data have been acquired only at heated conditions for the highest velocity case ($V_j/a = 1.2$) to avoid shock noise. Eight reservoir temperatures, ranging from $T_t/T_a = 1.0$ to 3.05 have been considered at each velocity, for this particular study. Utmost care is necessary, and has been exercised, in acquiring data at the lower velocities to avoid the Reynolds number effects and contamination by rig noise. The measured spectra at the eight conditions at each velocity were examined carefully and the spectral shapes compared with the similarity spectrum to detect the above two effects. During this exercise as well as in the analyses of spectra presented so far, an attempt was made to identify a critical Reynolds number that should be maintained to avoid the effects associated with Reynolds number. It has been found that there is no strict demarcating line that would delineate the Reynolds number below which a change in spectral shape (the extra hump noted in figures 9 and 10) occurs. Rather, there is a gradual change in spectral shape as Reynolds number decreases, as seen in figure 16(a). This trend is also suggested by the change in flow characteristics seen in figure 1. From a comprehensive analysis it has been found that, in general, a Reynolds number of ~400 000 would be adequate, while a value of 500 000 or more would be desirable. However, the transition spans a range of Reynolds number from ~300 000 to ~350 000. In the following figures, even though data were acquired at all eight combinations of NPR and temperature ratio at a particular jet velocity, only the test points that produced a Reynolds number of at least 335 000 have been included. Thus, any ambiguity in the results that may be attributed to the effects of Reynolds number is eliminated.

The overall power levels at each velocity, for several jet temperatures, are shown in figure 31. The velocities have been chosen carefully such that two of them are in the transition region where the power levels remain more or less constant, while there are two values each at higher and lower velocities. As seen in other measurements, the radiated power decreases with increasing temperature in the high-velocity regime (figures 31e and 31f). While the reduction is more pronounced at $V_j/a = 1.2$, the value is more modest at $V_j/a = 0.9$. Examination of figure 30 indicates that the noise picture is not clear-cut at $V_j/a = 0.9$. In the transition region, at velocities of 0.73 and 0.80 (figures 31c and 31d), the power level remains more or less constant for different jet temperatures. In the lower velocity regime (figures 31a and 31b) the trends are reversed, with the noise power increasing with increasing jet temperature. There were some questions about the older measurements at the lower velocities, which the current data has helped clarify. Hence, it is evident that the effect of jet temperature on the radiated noise is very different in different velocity regimes.

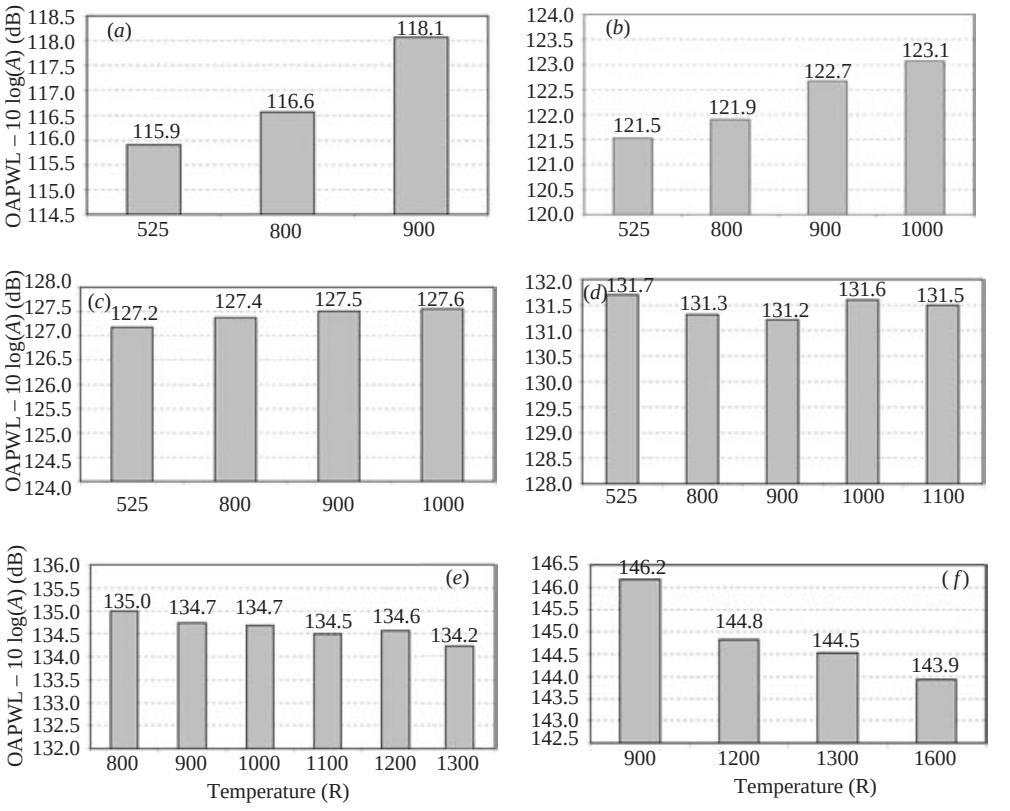

FIGURE 31. Variation of OAPWL with jet temperature. (*a*) $V_j/a = 0.53$; (*b*) 0.62; (*c*) 0.73; (*d*) 0.80; (*e*) 0.90; (*f*) 1.2.

The variation of the intensity of the radiated noise at 90°, where the contribution of the noise from large-scale structures is negligible, as a function of the acoustic Mach number is shown in figure 32. Again, the test points are grouped by temperature ratio. Least-square curve fits are shown for two cases, with $T_t/T_a = 1.0$ and 3.2. Let us concentrate our attention first in the supersonic regime ($V_j/a > 1.0$). There are clusters of data points at velocities of roughly 1.12, 1.24 and 1.37, with three points in each cluster. At these velocities, even though the hotter jets generate lower noise, the difference in levels is ~1 dB. Furthermore, the slopes of the curves (velocity exponents in this direction) decrease continuously as the jet temperature increases: from a value of 7.83 for the unheated case to 5.53 for $T_t/T_a = 3.2$. These trends are very similar to the ones observed for the overall power level, with the possibility that the hotter jets could radiate more noise in this direction at lower velocities. It is evident that the curves do not align themselves in parallel straight lines as proposed by Tam *et al.* (1996). The reduction in intensity due to heating is also lower than the value given by the formula in that reference. It should be noted that the formula is for peak amplitude and not intensity. However, since the shapes of the spectra are the same, the value of the intensity is related to that of the peak amplitude only by a scale factor. A similar variation of the intensities at 160° is shown in figure 33. As at 90°, there is a family of curves with decreasing slopes, which do not align themselves in parallel straight lines. The value of the velocity exponent

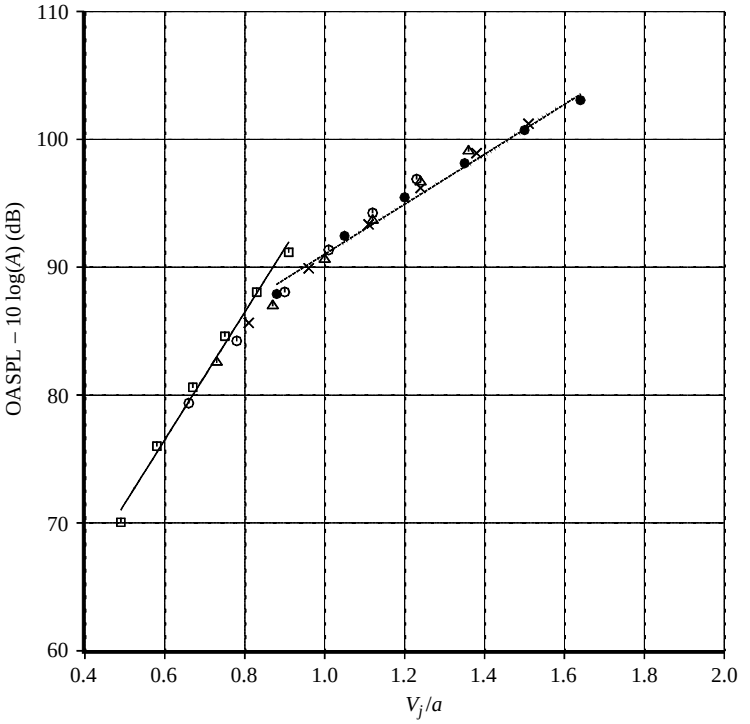

FIGURE 32. Variation of OASPL with jet velocity, $D = 2.45$ in. Angle $= 90°$. □, $T_t/T_a = 1.0$; ○, 1.8; △, 2.2; ×, 2.7; ●, 3.2.

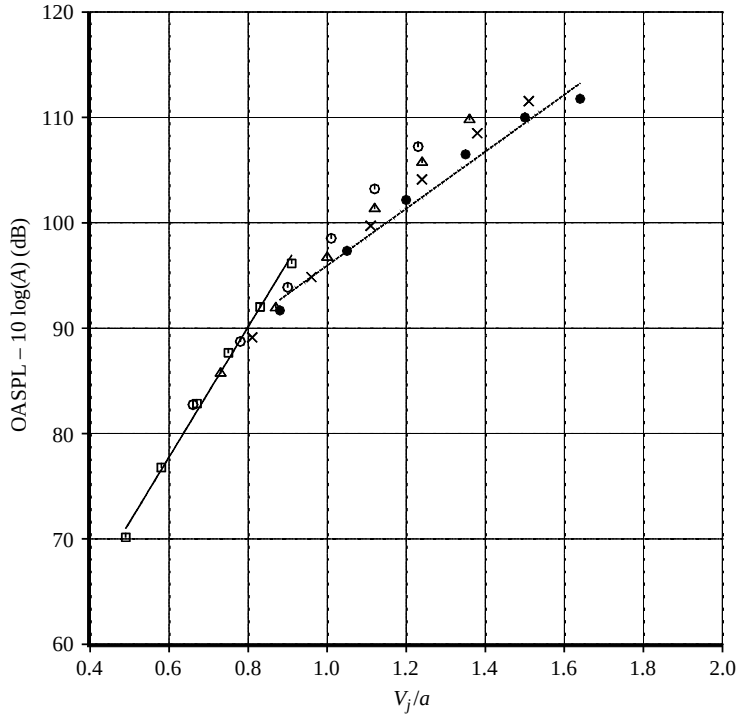

FIGURE 33. Variation of OASPL with jet velocity, $D = 2.45$ in. Angle $= 160°$. □, $T_t/T_a = 1.0$; ○, 1.8; △, 2.2; ×, 2.7; ●, 3.2.

again decreases as the jet temperature is increased, from a value of 9.67 for the unheated case to 7.67 for $T_t/T_a = 3.2$. At a constant jet velocity at supersonic acoustic Mach numbers, the reduction in level due to heating is more pronounced in the peak direction.

The effect of jet temperature on spectra, at fixed jet velocities, is now presented. The measured spectra at two angles of 90° and 150° for $V_j/a = 1.2$ and at three temperature ratios are shown in figures 34(*a*) and 34(*b*), respectively. The arrows in the figures denote the direction of increasing temperature. At both angles, there is a drop in the level across the entire spectrum as the jet temperature is increased, with the reduction more pronounced in the peak radiation direction. A similar comparison at $V_j/a = 0.73$, again at two angles of 90° and 155°, are shown in figures 35(*a*) and 35(*b*). At this velocity, there is little variation in the radiated power as seen in figure 31. The variations in spectral levels are also very small. As the jet temperature is increased, the spectral level at the lower frequencies increases while the level decreases at the higher frequencies at 90°. However, the change is ~1 dB or less. In the peak radiation direction, the magnitude of the change in level is even less. Thus, at this velocity, jets at different temperatures radiate the same levels of noise. Spectral variations at an acoustic Mach number of 0.62 are shown in figures 36(*a*) and 36(*b*), at 90° and 145°. As the jet temperature is increased, the amplitude at the lower frequencies and around the peak increases. At 90° there is no change in levels at the higher frequencies, while there is a minor change at the higher frequencies in the aft angle.

5. Conclusions

An experimental programme designed to clarify several outstanding issues on jet noise has been completed. The salient results of this study are enumerated below.

1. High-quality spectral data are absolutely vital, if one is not to be misled into favouring a particular theory or an explanation. The use of gross quantities such as OASPL or OAPWL for assessing the quality of data must be avoided. The difficulty of acquiring good data at low jet velocities has been emphasized through concrete examples.

2. Through the use of nozzles of different diameters, the effect of Reynolds number on acoustics has been established. It is shown that the spectral shape does change with increasing temperature, with an extra hump near the spectral peak, especially at lower Mach numbers. The observed change in spectral shape is shown to be an effect due to low Reynolds number. The link with Reynolds number has been identified for the first time here.

3. A critical value of the Reynolds number that would need to be maintained to avoid the effects associated with low Reynolds number has been estimated to be ~400 000. The increase in noise levels and a shift in the peak frequency to lower values at high jet temperatures, noted in low Reynolds number experiments, have been attributed to the contribution from dipoles by many researchers. The current results indicate that this hypothesis is erroneous and the observed increase in noise was due to the scale effect above and contamination by rig noise.

4. It is recognized that a few uncertainties still remain. It would be valuable to make clean spectral measurements at low jet velocities. This task, of course, is a great challenge. Detailed flow field measurements of the initial state of the boundary layer, turbulence measurements in the plume and optical observations would enhance our

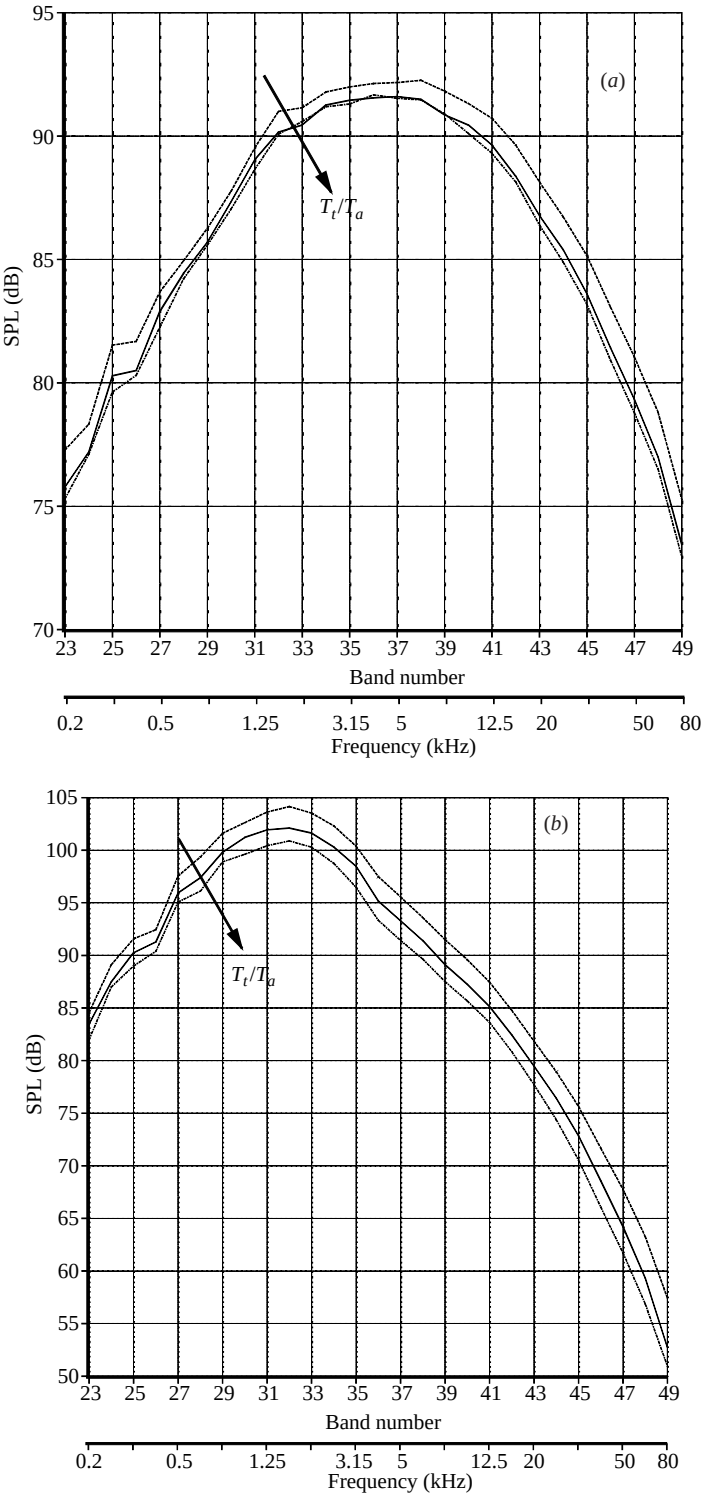

FIGURE 34. Variation of measured spectra with temperature at constant jet velocity, $D = 2.45$ in. $V_j/a = 1.2$. (*a*) Angle $= 90°$; (*b*) $150°$. Dashed line: $T_t/T_a = 1.71$; solid line: 2.29; dot-dashed: 3.05.

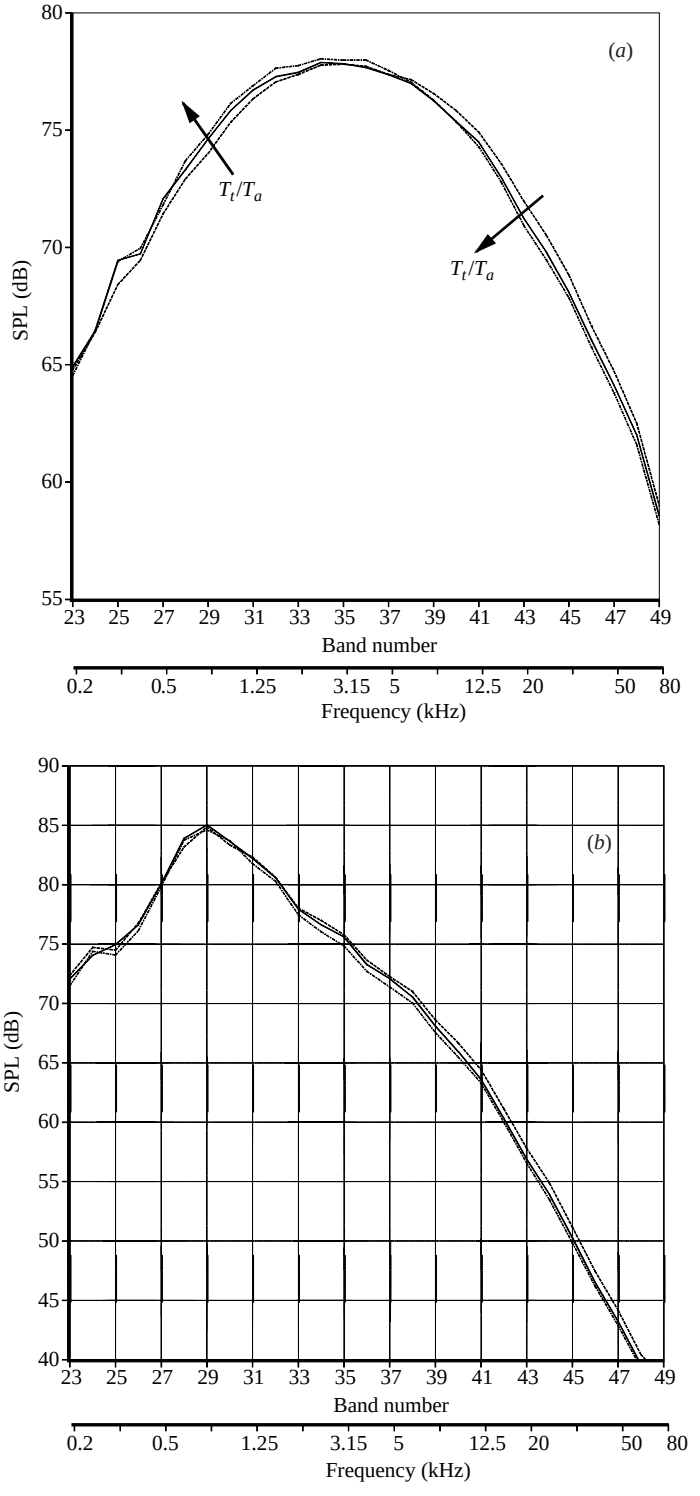

FIGURE 35. Variation of measured spectra with temperature at constant jet velocity, $D = 2.45$ in. $V_j/a = 0.73$. (*a*) Angle $= 90°$; (*b*) $155°$. Dashed line: $T_t/T_a = 1.51$; solid line: 1.71; dot-dashed: 1.90.

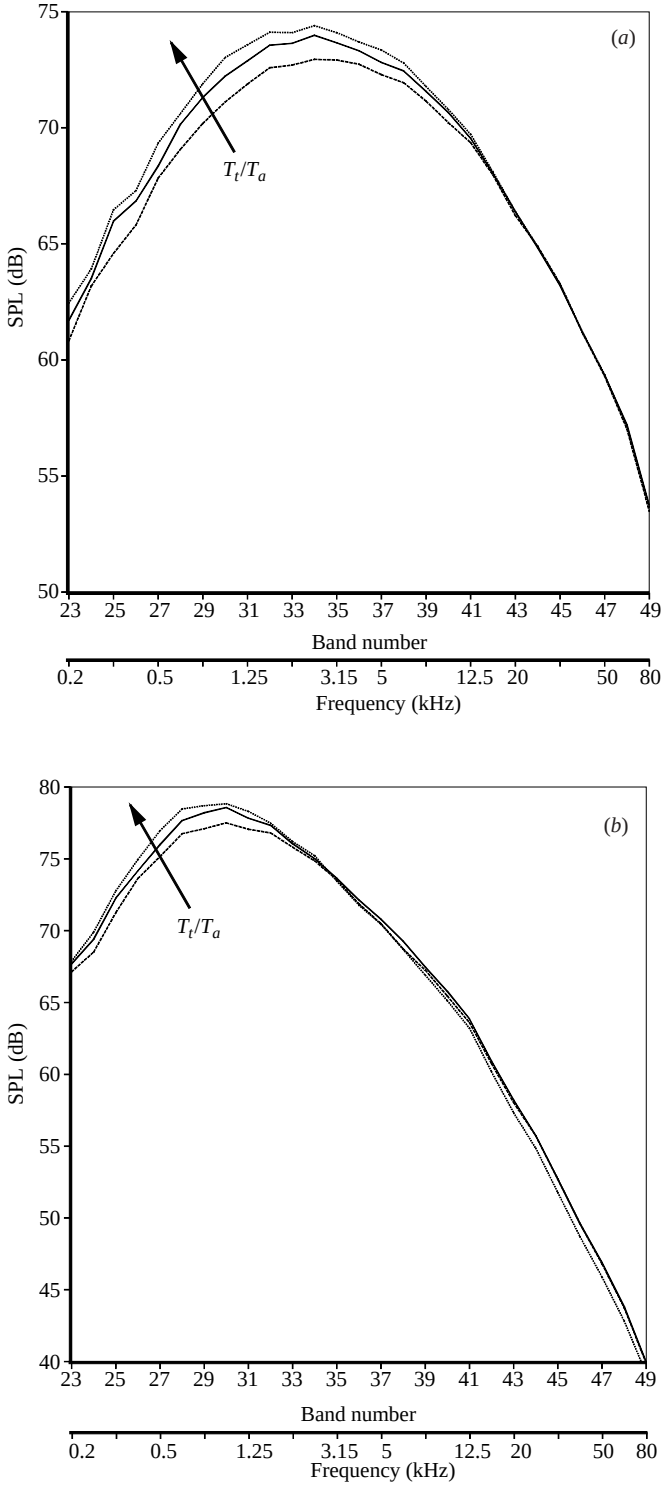

FIGURE 36. Variation of measured spectra with temperature at constant jet velocity, $D = 2.45$ in.. $V_j/a = 0.62$. (*a*) Angle = 90°; (*b*) 145°. Dashed line: $T_t/T_a = 1.51$; solid line: 1.71; dot-dashed: 1.90.

understanding and perhaps provide clues to the observed differences in the measured noise.

5. The spectral shapes in the forward quadrant and in the near-normal angles from unheated and heated subsonic jets are also shown to conform to the universal shape obtained from supersonic jet data. Thus, it has been established that the spectral shape at lower angles from unheated and heated jets at all (practical) Mach numbers is invariant and universal. This is an important result for the following reason: any jet noise theory or a model must predict this shape.

6. The spectral shape at large aft angles from unheated jets at low subsonic Mach numbers is shown to be the same as from highly heated jets at supersonic Mach numbers. This result is quite surprising and unexpected. Rapid decay of instability waves due to nonlinear mechanisms, just downstream of the potential core of the jet, is advanced as a possible mechanism for the observed trend at low jet Mach numbers.

7. When a subsonic jet is heated with the Mach number held constant, there is a broadening of the angular sector in which peak radiation occurs. Furthermore, there is a broadening of the spectral peak at aft angles. Similar trends have been observed at supersonic Mach numbers.

8. Just as for unheated jets, the peak frequency at angles close to the jet axis is independent of jet velocity as long as the acoustic Mach number (V_j/a) is less than unity. However, there is no general agreement on the mechanism that produces the change in spectral shape at large aft angles. Further study is required to resolve this issue.

9. The velocity exponent for radiated overall power has a weak dependence on temperature. Though the value of the exponent decreases with increasing temperature, a sixth-power dependence is not observed even at high temperatures. Using concrete examples, it has been demonstrated that the inclusion of contaminated data lowers the value of the velocity exponent.

10. The effect of jet temperature on noise, at fixed jet velocity, varies in different velocity regimes. While there is a decrease in noise levels at high velocities, the trends are reversed at lower velocities, with an intermediate range where the noise is insensitive to jet temperature. The current data confirm trends observed in previous studies.

It is a pleasure to thank Dr M. C. Joshi for several insightful comments and editorial suggestions and Professor P. J. Morris for clarifying certain issues. Several eminent technical suggestions by one of the anonymous reviewers helped to solidify the main conclusions of the paper. The author would like to express his sincere appreciation for the reviewer's efforts in this regard.

REFERENCES

Ahuja, K. K. 1973 Correlation and prediction of jet noise. *J. Sound Vib.* **29**, 155–168.

Ahuja, K. K. & Bushell, K. W. 1973 An experimental study of subsonic jet noise and comparison with theory. *J. Sound Vib.* **30**, 317–341.

Bushell, K. W. 1971 A survey of low velocity and coaxial jet noise with application to prediction. *J. Sound Vib.* **17**, 271–282.

Fisher, M. J., Lush, P. A. & Harper Bourne, M. 1973 Jet noise. *J. Sound Vib.* **28**, 563–585.

Goldstein, M. E. 2002 A unified appraoch to some recent developments in jet noise theory. *Intl J. Aeroacoust.* **1**, 1–16.

Hoch, R. G., Duponchel, J. P., Cocking, B. J. & Bryce, W. D. 1973 Studies of the influence of density on jet noise. *J. Sound Vib.* **28**, 649–668.

Lilley, G. M. 1996 The radiated noise from isotropic turbulence with applications to the theory of jet noise. *J. Sound Vib.* **190**, 463–476.

Lush, P. A. 1971 Measurements of subsonic jet noise and comparison with theory. *J. Fluid Mech.* **46**, 477–500.

Morfey, C. L., Szewczyk, V. M. & Tester, B. J. 1978 New scaling laws for hot and cold jet mixing noise based on a geometric acoustics model. *J. Sound Vib.* **61**, 255–292.

Morris, P. J. & Farassat, F. 2002 Acoustic analogy and alternative theories for jet noise prediction. *AIAA J.* **40**, 671–680.

Panda, J. & Seasholtz, R. G. 2002 Experimental investigation of desnsity fluctuations in high-speed jets and correlation with generated noise. *J. Fluid Mech.* **450**, 97–130.

Seiner, J. M., Ponton, M. K., Jansen, B. J. & Lagen, N. T. 1992 The effects of temperature on supersonic jet noise emission. *DGLR/AIAA Paper* 92-02-046.

Shields, F. D. & Bass, H. E. 1977 Atmospheric absorption of high frequency noise and application to fractional-octave band. *NASA CR* 2760.

Tam, C. K. W. 1991 Jet noise generated by large-scale coherent motion. In *Aeroacoustics of Flight Vehicles: Theory and Practice, Volume 1: Noise Sources* (ed. H. H. Hubbard). NASA RP-1258, pp. 311–390.

Tam, C. K. W. & Auriault, L. 1999 Jet mixing noise from fine-scale turbulence. *AIAA J.* **37**, 145–153.

Tam, C. K. W. & Burton, D. E. 1984 Sound generated by instability waves of supersonic flows. Part 1: Two dimensional mixing layers. Part 2. Axisymmetric jets. *J. Fluid Mech.* **138**, 249–295.

Tam, C. K. W. & Ganesan, A. 2003 A modified κ–ε turbulence model for calculating the mean flow and noise of hot jets. *AIAA Paper* 2003-1064.

Tam, C. K. W., Golebiowski, M. & Seiner, J. M. 1996 On the two components of turbulent mixing noise from supersonic jets. *AIAA Paper* 96-1716.

Tanna, H. K. 1977 An experimental study of jet noise. Part I: Turbulent mixing noise; Part II: Shock associate noise. *J. Sound Vib.* **50**, 405–444.

Tanna, H. K., Dean, P. D. & Fisher, M. J. 1975 The influence of temperature on shock-free supersonic jet noise. *J. Sound Vib.* **39**, 429–460.

Tester, B. J. & Morfey, C. L. 1976 Developments in jet noise modelling – theoretical predictions and comparisons with measured data. *J. Sound Vib.* **46**, 79–103.

Viswanathan, K. 2002 Analysis of the two similarity components of turbulent mixing noise. *AIAA J.* **40**, 1735–1744.

Viswanathan, K. 2003 Jet aeroacoustic testing: issues and implications. *AIAA J.* **41**, 1674–1689.